

# Exclusive diffractive production of photons in proton-proton collisions at the LHC

Piotr Lebiedowicz (IFJ PAN)

Otto Nachtmann (Univ. Heidelberg)

Antoni Szczurek (IFJ PAN)

based on

(1) arXiv: 2206.03411 [hep-ph], PRD106 (2022) 034023

(2) arXiv: 2208.12693 [hep-ph]

Plan:

- Introduction
- $pp \rightarrow pp$  and  $pp \rightarrow p p \gamma$   
in the tensor-pomeron model
- Soft Photon Approximation (SPA)
- Bremsstrahlung vs. CEP of photons,  
Results & Conclusions



THE HENRYK NIEWODNICZAŃSKI  
INSTITUTE OF NUCLEAR PHYSICS  
POLISH ACADEMY OF SCIENCES



UNIVERSITÄT  
HEIDELBERG  
ZUKUNFT  
SEIT 1386



Project No. BPN/BEK/2021/2/00009



New Vistas in Photon Physics  
in Heavy-Ion Collisions  
19-22 Sept 2022, Kraków, Poland,  
IFJ PAN & AGH University of Science  
and Technology

# Introduction

- The emission of soft photons, that is, photons of energy  $\omega \rightarrow 0$ , was treated in the seminal paper  
*F.E. Low, "Bremsstrahlung of very low-energy quanta in elementary particle collisions", Phys. Rev. 110 (1958) 974*

There it was shown that the term of order  $\omega^{-1}$  in the amplitude for the emission reaction can be obtained from the amplitude without photon emission. To this order the emission comes exclusively from the external particles. This is a strict consequence of QFT.

Many soft-photon approximations (SPAs) are based on this result.

- Experimental studies trying to verify Low's theorem have, in many cases, found large deviations from the SPA calculations. **see M. Völkl talk**
- More experimental (ALICE 3) and theoretical work is needed in order to clarify this “soft photon problem”.
- We started our investigations of soft-photon radiation with the processes:  $\pi^- \pi^0 \rightarrow \pi^- \pi^0 \gamma$ ,  $\pi^- \pi^+ \rightarrow \pi^- \pi^+ \gamma$   
*P.L. O. Nachtmann, A. Szczerba, PRD 105 (2022) 014022*  
We have discussed these reactions in the tensor-pomeron model. We have determined the kinematic regions where the SPAs are a good representation of our “standard” model result.  
[O. Nachtmann, “Photon emission in pion-pion scattering and Low's theorem revised”, see EMMI RRTF]  
in preparatory lectures
- Recently, we have considered soft-photon radiation in pp collisions:  $p^- p^+ \rightarrow p^- p^+ \gamma$   
*P.L. O. Nachtmann, A. Szczerba, “Soft-photon radiation in high-energy proton-proton collisions within the tensor-Pomeron approach: Bremsstrahlung”, PRD 106 (2022) 034023*

# Proton-proton scattering in the tensor-pomeron approach

We consider the reaction  $p(p_a) + p(p_b) \rightarrow p(p_1) + p(p_2)$

at high energies and small momentum transfer  $\sqrt{s} \gg m_p, \quad \sqrt{|t|} \lesssim m_p$ .

This is the kinematic region where the amplitudes are governed by the Regge exchanges.

We use the model developed in C. Ewerz, M. Maniatis, O. Nachtmann, Ann. Phys. 342 (2014) 31,  
“A model for soft high-energy scattering: tensor pomeron and vector odderon”.

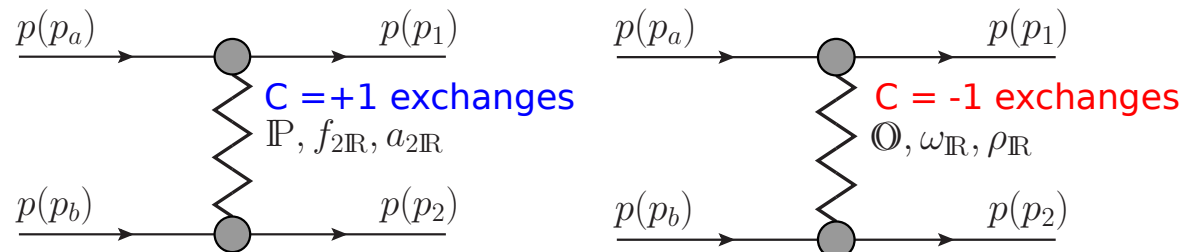
This model has a good basis from nonperturbative QCD considerations  
[O. Nachtmann, Ann. Phys. 209 (1991) 436].

We consider the usual Regge exchanges with charge conjugation  $C = +1$  and  $C = -1$ :

$C = +1$  pomeron (IP),  $f_2$  and  $a_2$  reggeons

$C = -1$  odderon (O),  $\omega$  and  $\rho$  reggeons

We assume that all  $C = +1$  exchange objects can be described as effective spin 2 symmetric tensor exchanges, all  $C = -1$  exchanges as effective vector exchanges.



- Effective propagator for tensor-pomeron exchange

$$i\Delta_{\mu\nu,\kappa\lambda}^{(\mathbb{P})}(s, t) = \frac{1}{4s} \left( g_{\mu\kappa}g_{\nu\lambda} + g_{\mu\lambda}g_{\nu\kappa} - \frac{1}{2}g_{\mu\nu}g_{\kappa\lambda} \right) (-is\alpha'_{\mathbb{P}})^{\alpha_{\mathbb{P}}(t)-1}$$

$$\alpha_{\mathbb{P}}(t) = \alpha_{\mathbb{P}}(0) + \alpha'_{\mathbb{P}}t, \quad \alpha_{\mathbb{P}}(0) = 1 + \epsilon_{\mathbb{P}} = 1.0808, \quad \alpha'_{\mathbb{P}} = 0.25 \text{ GeV}^{-2}$$

see e.g., A. Donnachie, H.G.Dosch, P.V.Landshoff, O.Nachtmann, "Pomeron Physics and QCD", CUP, 2002

- Effective proton-pomeron vertex

$$i\Gamma_{\mu\nu}^{(\mathbb{P}pp)}(p', p) = -i3\beta_{\mathbb{P}pp} F_1[(p' - p)^2] \left\{ \frac{1}{2} [\gamma_\mu(p' + p)_\nu + \gamma_\nu(p' + p)_\mu] - \frac{1}{4}g_{\mu\nu}(p' + p) \right\}$$

$$\beta_{\mathbb{P}pp} = 1.87 \text{ GeV}^{-1}$$

$$i\Gamma_{\mu\nu}^{(\mathbb{P}\bar{p}\bar{p})}(p', p) = i\Gamma_{\mu\nu}^{(\mathbb{P}pp)}(p', p)$$

We find from comparison to the TOTEM  $d\sigma/dt$  data:

- $\epsilon_{\mathbb{P}} = 0.0865$
- $F_1(t) \rightarrow F(t) = \exp(-b|t|)$  with  $b = 2.95 \text{ GeV}^{-2}$

- **Reaction  $pp \rightarrow pp$**

We discuss the reaction

$$p(p_a, \lambda_a) + p(p_b, \lambda_b) \rightarrow p(p_1, \lambda_1) + p(p_2, \lambda_2),$$

The momenta are indicated in brackets and  $\lambda_a, \lambda_b, \lambda_1, \lambda_2 \in \{1/2, -1/2\}$  are the helicity indices of the protons.

The kinematic variables are

$$s = (p_a + p_b)^2 = (p_1 + p_2)^2$$

$$t = (p_a - p_1)^2 = (p_b - p_2)^2$$

$$u = (p_a - p_2)^2 = (p_b - p_1)^2$$

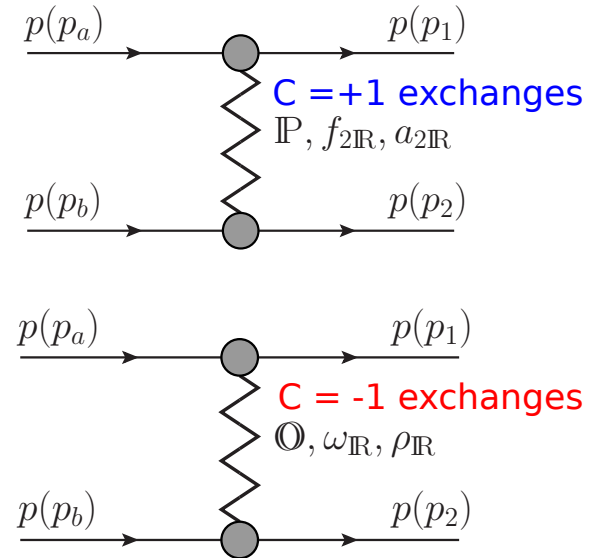
$$m_a^2 = p_a^2, m_b^2 = p_b^2, m_1^2 = p_1^2, m_2^2 = p_2^2$$

The interchange  $p_1 \leftrightarrow p_2$  implies  $t \leftrightarrow u$  where  $u = -s - t + m_a^2 + m_b^2 + m_1^2 + m_2^2$ .

We are interested in the kinematic region

$$\sqrt{s} \gg m_p, \quad \sqrt{|t|} \lesssim m_p, \quad s \gg |m_a^2|, |m_b^2|, |m_1^2|, |m_2^2|.$$

There we can neglect the diagrams with  $p_1 \leftrightarrow p_2$ .



- **Off-shell  $pp$  elastic scattering amplitude**

We use tensor-product notation.

The first factors will always refer to the  $p_a-p_1$  line, the second to the  $p_b-p_2$  line.

$$\begin{aligned}\mathcal{M}^{(0)}(p_a, p_b, p_1, p_2) &= \mathcal{M}_{\mathbb{P}}^{(0)} + \mathcal{M}_{f_{2\mathbb{R}}}^{(0)} + \mathcal{M}_{a_{2\mathbb{R}}}^{(0)} + \mathcal{M}_{\mathbb{O}}^{(0)} + \mathcal{M}_{\omega_{\mathbb{R}}}^{(0)} + \mathcal{M}_{\rho_{\mathbb{R}}}^{(0)} \\ &= i\mathcal{F}_T(s, t) [\gamma^\mu \otimes \gamma_\mu(p_a + p_1, p_b + p_2) + (\not{p}_b + \not{p}_2) \otimes (\not{p}_a + \not{p}_1) - \frac{1}{2}(\not{p}_a + \not{p}_1) \otimes (\not{p}_b + \not{p}_2)] - \mathcal{F}_V(s, t) \gamma^\mu \otimes \gamma_\mu\end{aligned}$$

where  $\mathcal{F}_T(s, t) = \mathcal{F}_{\mathbb{P}pp}(s, t) + \mathcal{F}_{f_{2\mathbb{R}}pp}(s, t) + \mathcal{F}_{a_{2\mathbb{R}}pp}(s, t)$   
 $\mathcal{F}_V(s, t) = \mathcal{F}_{\mathbb{O}pp}(s, t) + \mathcal{F}_{\omega_{\mathbb{R}}pp}(s, t) + \mathcal{F}_{\rho_{\mathbb{R}}pp}(s, t)$

and  $\mathcal{F}_{\mathbb{P}pp}(s, t) = [3\beta_{\mathbb{P}pp} F(t)]^2 \frac{1}{4s} (-is\alpha'_{\mathbb{P}})^{\alpha_{\mathbb{P}}(t)-1}$

- **On-shell  $pp$  elastic scattering amplitude**

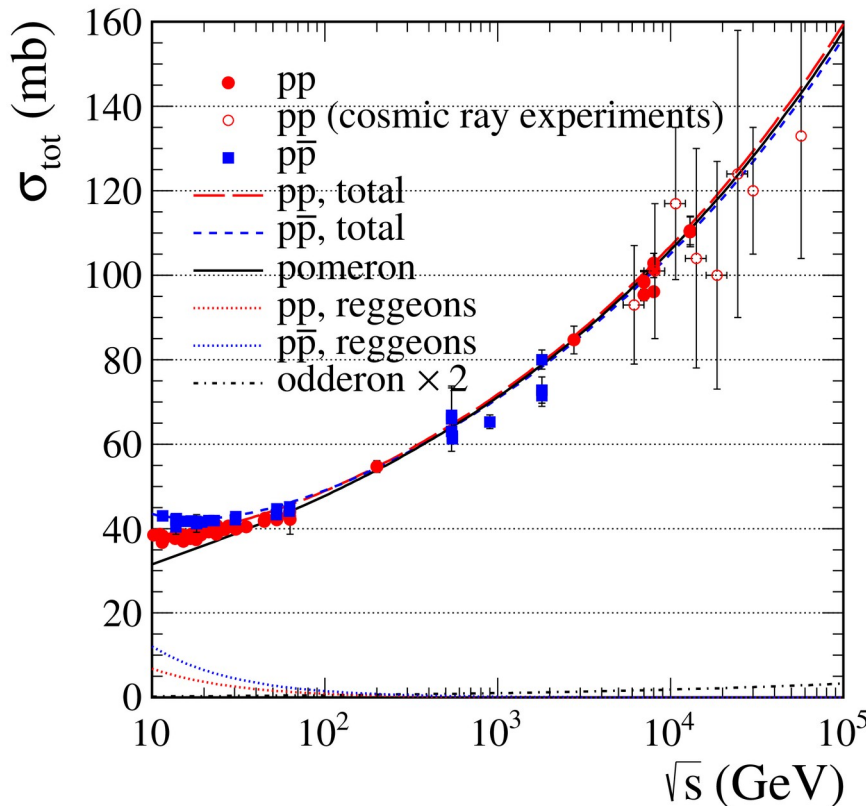
$$\begin{aligned}\langle p(p_1, \lambda_1), p(p_2, \lambda_2) | \mathcal{T} | p(p_a, \lambda_a), p(p_b, \lambda_b) \rangle &\equiv \mathcal{M}^{(\text{on shell}) pp}(s, t) \\ &= \bar{u}_1 \otimes \bar{u}_2 \mathcal{M}^{(0)}(p_a, p_b, p_1, p_2) u_a \otimes u_b|_{\text{on shell}} \\ &= i\mathcal{F}_T(s, t) [\bar{u}_1 \gamma^\mu u_a \bar{u}_2 \gamma_\mu u_b (p_a + p_1, p_b + p_2) + \bar{u}_1 \gamma^\mu u_a (p_b + p_2)_\mu \bar{u}_2 \gamma^\nu u_b (p_a + p_1)_\nu - 2m_p^2 \bar{u}_1 u_a \bar{u}_2 u_b] \\ &\quad - \mathcal{F}_V(s, t) \bar{u}_1 \gamma^\mu u_a \bar{u}_2 \gamma_\mu u_b\end{aligned}$$

where  $\bar{u}_1 = \bar{u}(p_1, \lambda_1)$ ,  $u_a = u(p_a, \lambda_a)$ , etc.

- **Comparison of the model with the total cross section data**

The total cross section for unpolarised protons, obtained from the forward-scattering amplitudes using the optical theorem, is

$$\sigma_{\text{tot}}(pp) = \frac{1}{\sqrt{s(s - 4m_p^2)}} \frac{1}{4} \sum_{\lambda_a, \lambda_b} \text{Im} \langle p(p_a, \lambda_a), p(p_b, \lambda_b) | \mathcal{T} | p(p_a, \lambda_a), p(p_b, \lambda_b) \rangle$$



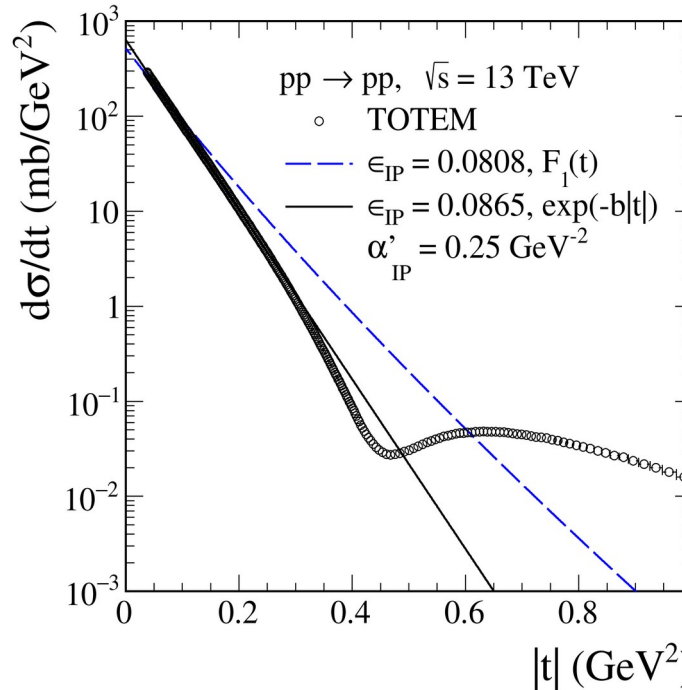
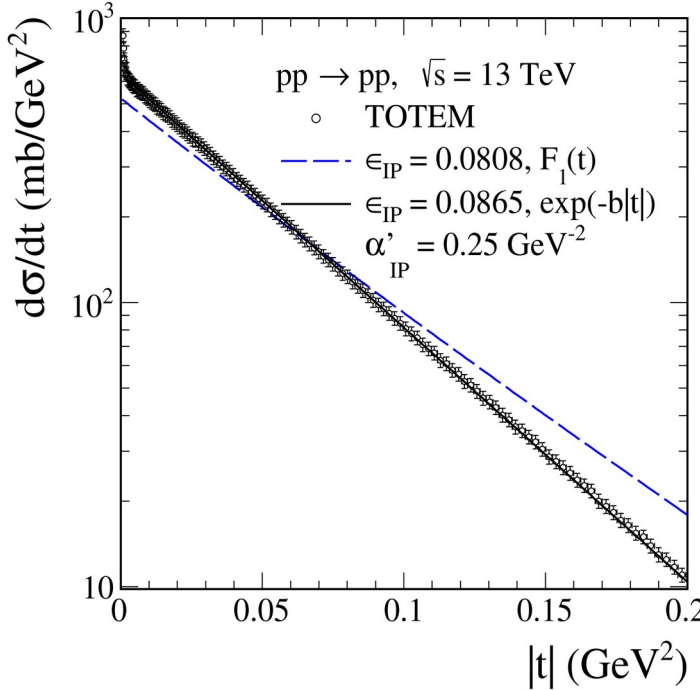
The high-energy cross section is dominated by the pomeron exchange.

The regeon and odderon effects are very small. We get for large energies a total cross section for  $pp$  exceeding that for  $p\bar{p}$  collisions,  
 $\sigma_{\text{tot}}(pp) > \sigma_{\text{tot}}(p\bar{p})$ .

We only need a reasonable description of the data for  $\sqrt{s} = 13$  TeV as a prerequisite for the calculation of photon radiation in  $pp$  collisions.

- **Comparison of the model with elastic  $pp$  differential cross section data measured by TOTEM**

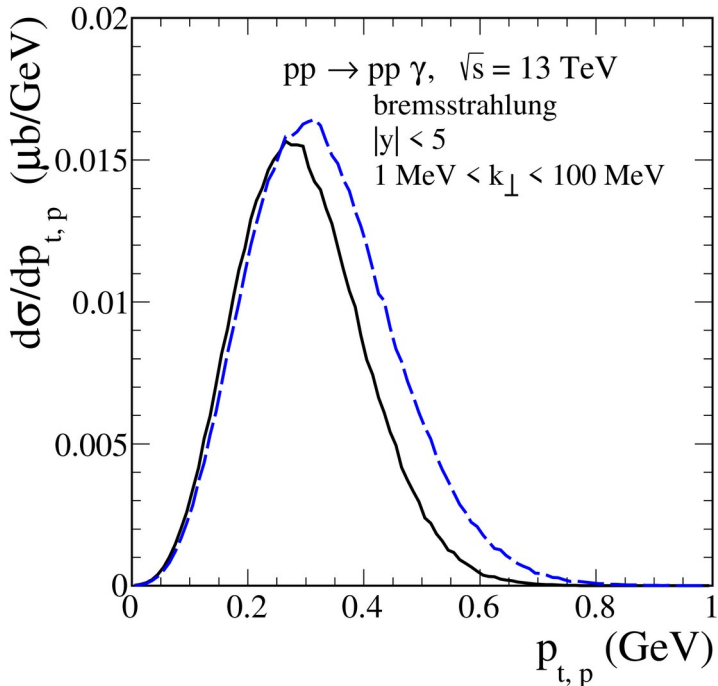
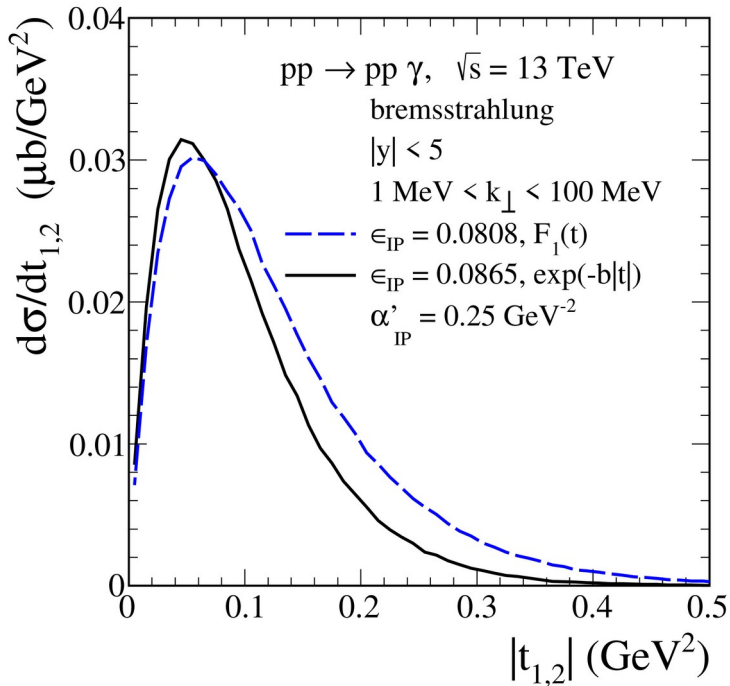
[G. Antchev et al. (TOTEM Collaboration), Eur. Phys. J. C79 (2019) 785, Eur. Phys. J. C79 (2019) 861]



There are also NEW  
ATLAS results @ 13 TeV  
→ see R. Staszewski talk

- We find a good description of the data in the region  $0.003 \text{ GeV}^2 \leq -t \leq 0.26 \text{ GeV}^2$  with our single-pomeron exchange model with  $\epsilon_{IP} = 0.0865$  and  $F(t) = \exp(-b|t|)$ ,  $b = 2.95 \text{ GeV}^{-2}$
- For comparison, we show also the results for  $\epsilon_{IP} = 0.0808$  and the Dirac form factor  $F_1(t)$
- In order to produce the dip one needs the interference of various terms in the amplitude, at least three terms: IP + IPIP + ggg [see, e.g., Donnachie and Landshoff, PLB 727 (2013) 500]
- The so-called “break effect”, which leads to a smooth deflection of the linear exponential behavior of the diffractive cone should also be included [see L. Jenkovszky, I. Szanyi, C.-I. Tan, EPJA54 (2018) 116] 8

- Results for  $pp \rightarrow pp\gamma$  reaction (diffractive bremsstrahlung)



- The distributions in four-momentum transfer squared  $|t_{1,2}|$  where  $t_{1,2}$  is either  $t_1$  or  $t_2$  and in transverse momentum of the outgoing proton  $p_{t,p}$  for the reaction  $pp \rightarrow pp\gamma$
- We see that photons come predominantly from  $pp$  collisions with momentum transfers between the protons of order  $p_{t,p} \sim \sqrt{|t_{1,2}|} \sim 0.3$  GeV

## Proton-proton scattering with photon emission

We consider  $p(p_a, \lambda_a) + p(p_b, \lambda_b) \rightarrow p(p'_1, \lambda_1) + p(p'_2, \lambda_2) + \gamma(k, \epsilon)$ .

The momenta are denoted by  $p_a, \dots, k$ , the helicities of the protons by  $\lambda_a, \dots, \lambda_2$ , and  $\epsilon$  is the polarisation vector of the photon.

The relevant  $\mathcal{T}$ -matrix element is

$$\langle p(p'_1, \lambda_1), p(p'_2, \lambda_2), \gamma(k, \epsilon) | \mathcal{T} | p(p_a, \lambda_a), p(p_b, \lambda_b) \rangle = (\epsilon^\mu)^* \mathcal{M}_\mu^{(\text{total})}(p_a, \lambda_a; p_b, \lambda_b; p'_1, \lambda_1; p'_2, \lambda_2; k).$$

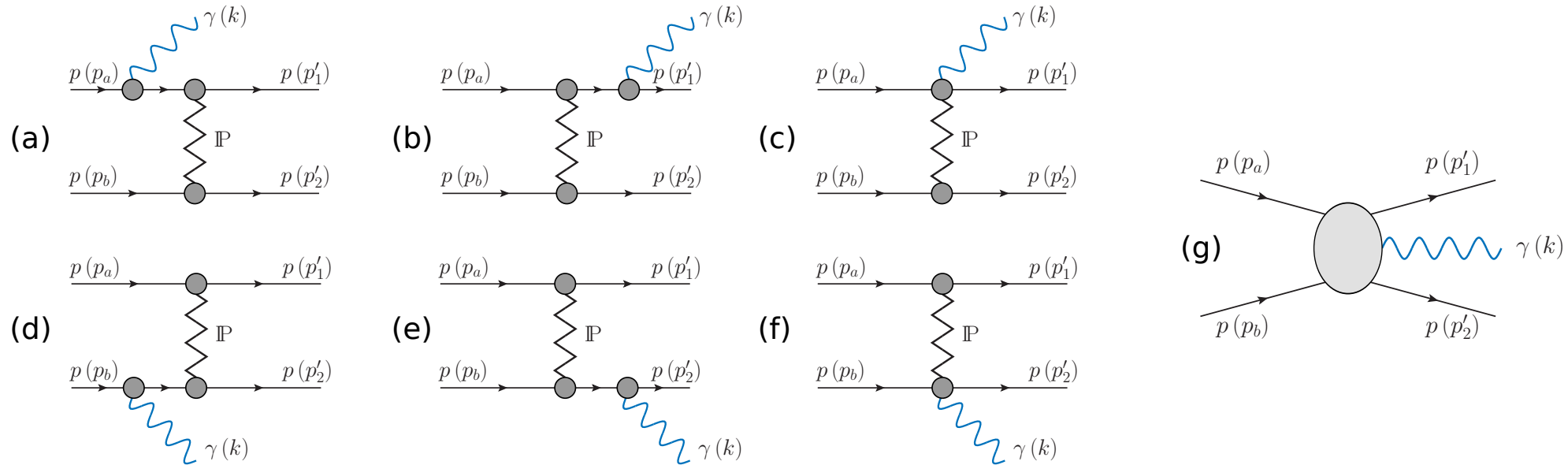
The complete amplitude is  $\mathcal{M}_\mu^{(\text{total})} = \mathcal{M}_\mu(p'_1, p'_2) - \mathcal{M}_\mu(p'_2, p'_1)$ .

The relative minus sign here is due to the Fermi statistics, which requires the amplitude to be antisymmetric under interchange of the two final protons. For diffractive scattering the amplitude  $\mathcal{M}_\mu(p'_2, p'_1)$  can be neglected.

Therefore, we get with very accuracy, the inclusive cross section for the real-photon yield

$$\begin{aligned} d\sigma(pp \rightarrow pp\gamma) &= \frac{1}{2\sqrt{s(s-4m_p^2)}} \frac{d^3k}{(2\pi)^3 2k^0} \int \frac{d^3p'_1}{(2\pi)^3 2p'^0_1} \frac{d^3p'_2}{(2\pi)^3 2p'^0_2} (2\pi)^4 \delta^{(4)}(p'_1 + p'_2 + k - p_a - p_b) \\ &\quad \times \frac{1}{4} \sum_{p \text{ spins}} \mathcal{M}_\mu(p'_1, p'_2) (\mathcal{M}_\nu(p'_1, p'_2))^*(-g^{\mu\nu}) \quad \text{where } \sum_{\lambda_\gamma} (\epsilon^\mu(k, \lambda_\gamma))^* \epsilon^\nu(k, \lambda_\gamma) = -g^{\mu\nu} \end{aligned}$$

- **Diagrams for the reaction  $pp \rightarrow pp\gamma$**



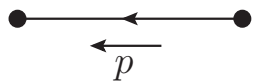
We have 7 types of diagrams. In the diagrams (a), (b), (d), and (e) the photon is emitted from the external proton lines. The diagrams (c) and (f) correspond to contact terms. [We shall call the diagrams \(a\), \(b\), \(d\), \(e\), made gauge invariant by the addition of \(c\) and \(f\), the bremsstrahlung diagrams.](#) All “anomalous” terms are subsumed in (g) (structure term).

Our “standard” (diffractive photon-bremsstrahlung) amplitude is

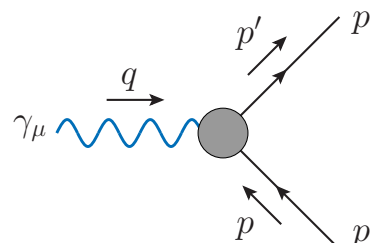
$$\mathcal{M}_\mu^{(\text{standard})} = \mathcal{M}_\mu^{(a)} + \mathcal{M}_\mu^{(b)} + \mathcal{M}_\mu^{(c)} + \mathcal{M}_\mu^{(d)} + \mathcal{M}_\mu^{(e)} + \mathcal{M}_\mu^{(f)}$$

The amplitude must satisfy the gauge-invariant relation  $k^\mu \mathcal{M}_\mu^{(\text{standard})} = 0$

- We use the following standard proton propagator and  $\gamma pp$  vertex:



$$iS_F(p) = \frac{i}{\not{p} - m_p + i\epsilon} = i \frac{\not{p} + m_p}{p^2 - m_p^2 + i\epsilon}$$



$$i\Gamma_\mu^{(\gamma pp)}(p', p) = -ie[F_1(0)\gamma_\mu + \frac{i}{2m_p}\sigma_{\mu\nu}q^\nu F_2(0)]$$

$$F_1(0) = 1$$

$$F_2(0) = \left(\frac{\mu_p}{\mu_N} - 1\right), \quad \mu_N = \frac{e}{2m_p}, \quad \frac{\mu_p}{\mu_N} = 2.7928$$

$$e > 0, \quad e = \sqrt{4\pi\alpha_{\text{em}}}$$

We take the form factors at  $q^2 = 0$  in order to be consistent with the Ward-Takahashi identity:

$$(p' - p)^\mu \Gamma_\mu^{(\gamma pp)}(p', p) = -e[S_F^{-1}(p') - S_F^{-1}(p)]$$

We are interested in real photon emission where  $k = -q$ ,  $k^2 = q^2 = 0$ .

- The kinematic variables for the  $pp \rightarrow pp\gamma$  reaction are:

$$s = (p_a + p_b)^2 = (p'_1 + p'_2 + k)^2$$

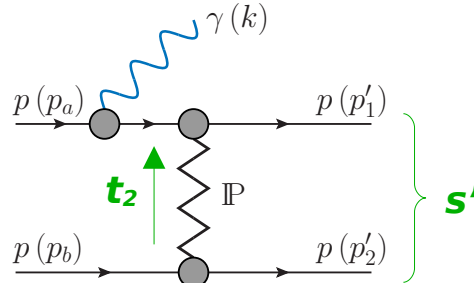
$$s' = (p_a + p_b - k)^2 = (p'_1 + p'_2)^2$$

$$t_1 = (p_a - p'_1)^2 = (p_b - p'_2 - k)^2$$

$$t_2 = (p_b - p'_2)^2 = (p_a - p'_1 - k)^2$$

- We get with the **off-shell scattering amplitudes** for diagrams (a) and (b):

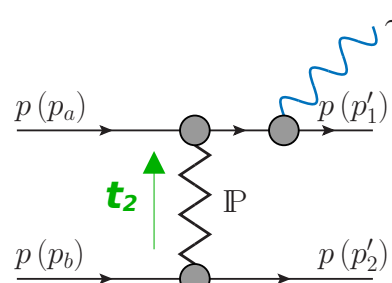
(a)



$$\mathcal{M}_\mu^{(a)}$$

$$\begin{aligned} &= -\bar{u}_{1'} \otimes \bar{u}_{2'} \mathcal{M}^{(0)}(p_a - k, p_b, p'_1, p'_2) [S_F(p_a - k) \Gamma_\mu^{(\gamma pp)}(p_a - k, p_a) u_a] \otimes u_b \\ &= e \bar{u}_{1'} \otimes \bar{u}_{2'} \left\{ i \mathcal{F}_T(s', t_2) [\gamma^\alpha \otimes \gamma_\alpha(p_a - k + p'_1, p_b + p'_2) + (\not{p}_b + \not{p}'_2) \otimes (\not{p}_a - \not{k} + \not{p}'_1) \right. \\ &\quad \left. - \frac{1}{2} (\not{p}_a - \not{k} + \not{p}'_1) \otimes (\not{p}_b + \not{p}'_2)] - \mathcal{F}_V(s', t_2) \gamma^\alpha \otimes \gamma_\alpha \right\} \\ &\quad \times \left[ \frac{\not{p}_a - \not{k} + m_p}{(p_a - k)^2 - m_p^2 + i\varepsilon} \left( \gamma_\mu - \frac{i}{2m_p} \sigma_{\mu\nu} k^\nu F_2(0) \right) u_a \right] \otimes u_b \end{aligned}$$

(b)



$$\mathcal{M}_\mu^{(b)}$$

$$\begin{aligned} &= -[\bar{u}_{1'} \Gamma_\mu^{(\gamma pp)}(p'_1, p'_1 + k) S_F(p'_1 + k)] \otimes \bar{u}_{2'} \mathcal{M}^{(0)}(p_a, p_b, p'_1 + k, p'_2) u_a \otimes u_b \\ &= e [\bar{u}_{1'} \left( \gamma_\mu - \frac{i}{2m_p} \sigma_{\mu\nu} k^\nu F_2(0) \right) \frac{\not{p}'_1 + \not{k} + m_p}{(p'_1 + k)^2 - m_p^2 + i\varepsilon}] \otimes \bar{u}_{2'} \\ &\quad \times \left\{ i \mathcal{F}_T(s, t_2) [\gamma^\alpha \otimes \gamma_\alpha(p_a + p'_1 + k, p_b + p'_2) + (\not{p}_b + \not{p}'_2) \otimes (\not{p}_a + \not{p}'_1 + \not{k}) \right. \\ &\quad \left. - \frac{1}{2} (\not{p}_a + \not{p}'_1 + \not{k}) \otimes (\not{p}_b + \not{p}'_2)] - \mathcal{F}_V(s, t_2) \gamma^\alpha \otimes \gamma_\alpha \right\} u_a \otimes u_b \end{aligned}$$

Using the Ward-Takahashi identity we find

$$\begin{aligned} k^\mu \mathcal{M}_\mu^{(a)} &= -e \bar{u}_{1'} \otimes \bar{u}_{2'} \mathcal{M}^{(0)}(p_a - k, p_b, p'_1, p'_2) u_a \otimes u_b, \\ k^\mu \mathcal{M}_\mu^{(b)} &= e \bar{u}_{1'} \otimes \bar{u}_{2'} \mathcal{M}^{(0)}(p_a, p_b, p'_1 + k, p'_2) u_a \otimes u_b. \end{aligned}$$

Now we impose the gauge invariance condition which must hold also for the photon emission from the  $p_a$ - $p'_1$  lines in (a – c) diagrams alone:

$$k^\mu (\mathcal{M}_\mu^{(a)} + \mathcal{M}_\mu^{(b)} + \mathcal{M}_\mu^{(c)}) = 0.$$

We obtain then:

$$\begin{aligned} k^\mu \mathcal{M}_\mu^{(c)} &= -k^\mu \mathcal{M}_\mu^{(a)} - k^\mu \mathcal{M}_\mu^{(b)} \\ &= e \bar{u}_{1'} \otimes \bar{u}_{2'} [\mathcal{M}^{(0)}(p_a - k, p_b, p'_1, p'_2) - \mathcal{M}^{(0)}(p_a, p_b, p'_1 + k, p'_2)] u_a \otimes u_b \end{aligned}$$

We get

$$\begin{aligned} \mathcal{M}_\mu^{(c)} &= e \bar{u}_{1'} \otimes \bar{u}_{2'} \left\{ -i \mathcal{F}_T(s, t_2) [2\gamma^\alpha \otimes \gamma_\alpha (p_b + p'_2)_\mu + 2(\not{p}_b + \not{p}'_2) \otimes \gamma_\mu - \gamma_\mu \otimes (\not{p}_b + \not{p}'_2)] \right. \\ &\quad + i \frac{(2p_a + 2p_b - k)_\mu}{s} \Delta \mathcal{F}_T(s, t_2, \kappa) [\gamma^\alpha \otimes \gamma_\alpha (p_a + p'_1 - k, p_b + p'_2) + (\not{p}_b + \not{p}'_2) \otimes (\not{p}_a + \not{p}'_1 - \not{k}) - \frac{1}{2} (\not{p}_a + \not{p}'_1 - \not{k}) \otimes (\not{p}_b + \not{p}'_2)] \\ &\quad \left. - \frac{(2p_a + 2p_b - k)_\mu}{s} \Delta \mathcal{F}_V(s, t_2, \kappa) \gamma^\alpha \otimes \gamma_\alpha \right\} u_a \otimes u_b. \end{aligned}$$

We rewrite the amplitude  $\mathcal{M}_\mu^{(a+b+c)} = \mathcal{M}_\mu^{(a)} + \mathcal{M}_\mu^{(b)} + \mathcal{M}_\mu^{(c)}$ ,  
in a way which is more suitable for numerical computations.

We use the following relations:

$$\begin{aligned} & \frac{\not{p}_a - \not{k} + m_p}{(p_a - k)^2 - m_p^2 + i\varepsilon} \left( \gamma_\mu - \frac{i}{2m_p} \sigma_{\mu\nu} k^\nu \textcolor{magenta}{F}_2(0) \right) u_a \\ &= \frac{1}{-2p_a \cdot k + k^2 + i\varepsilon} \left\{ 2p_{a\mu} - k_\mu + (k_\mu - \not{k}\gamma_\mu) + \frac{\textcolor{magenta}{F}_2(0)}{2m_p} [2(p_{a\mu} \not{k} - (p_a \cdot k)\gamma_\mu) + 2m_p(k_\mu - \not{k}\gamma_\mu) - (\not{k}k_\mu - k^2\gamma_\mu)] \right\} u_a \end{aligned}$$

$$\begin{aligned} & \bar{u}_{1'} \left( \gamma_\mu - \frac{i}{2m_p} \sigma_{\mu\nu} k^\nu \textcolor{magenta}{F}_2(0) \right) \frac{\not{p}'_1 + \not{k} + m_p}{(p'_1 + k)^2 - m_p^2 + i\varepsilon} \\ &= \bar{u}_{1'} \frac{1}{2p'_1 \cdot k + k^2 + i\varepsilon} \left\{ 2p'_{1\mu} + k_\mu - (k_\mu - \gamma_\mu \not{k}) + \frac{\textcolor{magenta}{F}_2(0)}{2m_p} [-2(p'_{1\mu} \not{k} - (p'_1 \cdot k)\gamma_\mu) - 2m_p(k_\mu - \gamma_\mu \not{k}) - (k_\mu \not{k} - k^2\gamma_\mu)] \right\} \end{aligned}$$

Exploiting the properties of the Dirac spinors,  
 $\not{p}_a u_a = m_p u_a$ ,  $\bar{u}_{1'} \not{p}'_1 = \bar{u}_{1'} m_p$  etc., we can write

$$\mathcal{M}_\mu^{(\text{standard})} = \sum_{j=1}^7 (\mathcal{M}_{T,\mu}^{(a+b+c)j} + \mathcal{M}_{T,\mu}^{(d+e+f)j}) + \sum_{j'=1}^4 (\mathcal{M}_{V,\mu}^{(a+b+c)j'} + \mathcal{M}_{V,\mu}^{(d+e+f)j'}).$$

Here T and V stand for the tensor- and vector-exchange diagrams, respectively,  
and  $j$  and  $j'$  are just labels for the subamplitudes in the sums.

For  $j = 1, 2, 4$  we have

$$\begin{aligned} \mathcal{M}_{T,\mu}^{(a+b+c)1} &= e\bar{u}_{1'} \otimes \bar{u}_{2'} \left\{ i\mathcal{F}_T(s, t_2) [\gamma^\alpha \otimes \gamma_\alpha(p_a + p'_1, p_b + p'_2) + (\not{p}_b + \not{p}'_2) \otimes (\not{p}_a + \not{p}'_1) - 2m_p^2 1 \otimes 1] \right. \\ &\quad \times \left[ \frac{2p_{a\mu} - k_\mu}{-2p_a \cdot k + k^2 + i\varepsilon} + \frac{2p'_{1\mu} + k_\mu}{2p'_1 \cdot k + k^2 + i\varepsilon} \right] \} u_a \otimes u_b \end{aligned}$$

The amplitudes  $j = 1$  contain the pole term  $\propto 1/\omega$  for  $\omega \rightarrow 0$ .

$$\begin{aligned} \mathcal{M}_{T,\mu}^{(a+b+c)2} &= e\bar{u}_{1'} \otimes \bar{u}_{2'} \left\{ i\mathcal{F}_T(s', t_2) \frac{1}{-2p_a \cdot k + k^2 + i\varepsilon} \right. \\ &\quad \times [\gamma^\alpha \otimes \gamma_\alpha(p_a + p'_1 - k, p_b + p'_2) + (\not{p}_b + \not{p}'_2) \otimes (\not{p}_a + \not{p}'_1 - \not{k})] \\ &\quad \times [k_\mu - \not{k}\gamma_\mu + \frac{\textcolor{violet}{F}_2(0)}{2m_p} (2p_{a\mu} \not{k} - 2(p_a \cdot k)\gamma_\mu + 2m_p(k_\mu - \not{k}\gamma_\mu) - (\not{k}k_\mu - k^2\gamma_\mu))] \otimes 1 \} u_a \otimes u_b \end{aligned}$$

$$\begin{aligned} \mathcal{M}_{T,\mu}^{(a+b+c)4} &= e\bar{u}_{1'} \otimes \bar{u}_{2'} \left\{ i\mathcal{F}_T(s, t_2) \frac{1}{2p'_1 \cdot k + k^2 + i\varepsilon} \right. \\ &\quad \times [-(k_\mu - \gamma_\mu \not{k}) + \frac{\textcolor{violet}{F}_2(0)}{2m_p} (-2p'_{1\mu} \not{k} + 2(p'_1 \cdot k)\gamma_\mu - 2m_p(k_\mu - \gamma_\mu \not{k}) - (k_\mu \not{k} - k^2\gamma_\mu))] \otimes 1 \\ &\quad \times [\gamma^\alpha \otimes \gamma_\alpha(p_a + p'_1 + k, p_b + p'_2) + (\not{p}_b + \not{p}'_2) \otimes (\not{p}_a + \not{p}'_1 + \not{k})] \} u_a \otimes u_b \end{aligned}$$

We have

$$\mathcal{M}_{T,\mu}^{(d+e+f)j} = \mathcal{M}_{T,\mu}^{(a+b+c)j} \Big|_{\substack{(p_a, \lambda_a) \leftrightarrow (p_b, \lambda_b) \\ (p'_1, \lambda_1) \leftrightarrow (p'_2, \lambda_2)}} \quad \text{for } j = 1, \dots, 7$$

where we also exchange the order of the tensor products.

All subamplitudes are separately gauge invariant:

$$k^\mu \mathcal{M}_{T,\mu}^{(a+b+c)j} = 0$$

$$k^\mu \mathcal{M}_{T,\mu}^{(d+e+f)j} = 0$$

- The term  $j = 1$  has singularity for  $\omega \rightarrow 0$ .
- The terms  $j = 2$  and  $4$  have no singularity for  $\omega \rightarrow 0$ .  
The main term here comes from the anomalous magnetic moment  $F_2(0)$ .
- Thus, the term  $j = 1$  will win over the  $2$  and  $4$  terms individually for  $\omega \rightarrow 0$ .

We find that the pole term ( $j = 1$ ) only dominates over these non-singular terms individually for very small  $k_\perp$ :

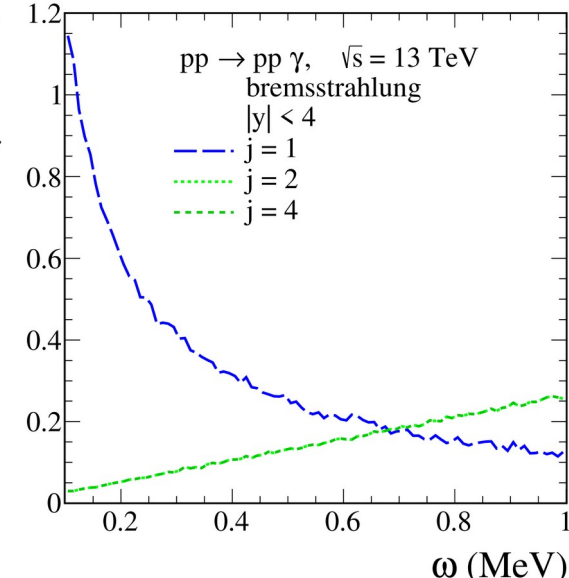
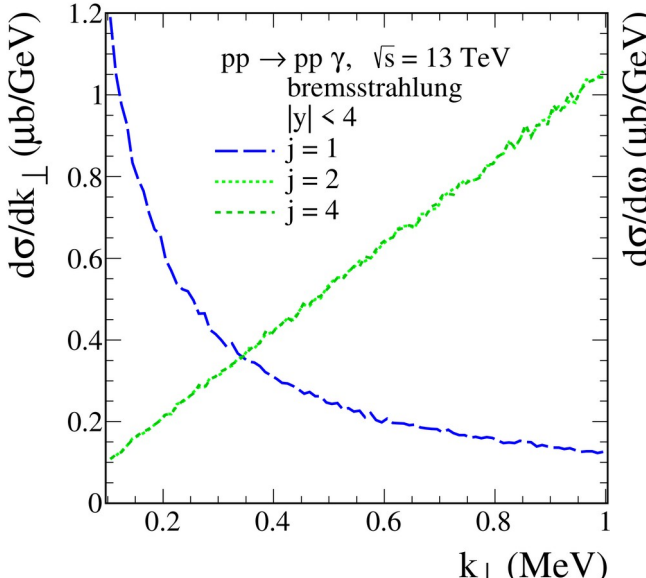
$$k_\perp \approx \omega \lesssim 2m_p^2/\sqrt{s} \cong 0.15 \text{ MeV}$$

Explicit calculations confirm the order of magnitude of this estimate.

- In the literature such small values for  $\omega$  as a limit for the dominance of the  $\omega^{-1}$  term are mentioned.  
In [V. Del Duca, High-energy bremsstrahlung theorems for soft photons, Nucl.Phys.B 345 (1990) 369] it is argued that for **hard** high-energy elastic processes Low's original result gives a reliable representation of the radiative amplitude only in the vanishingly small region  $\omega \lesssim m^2/Q$  in the limit  $Q \rightarrow \infty$ .  
Here  $Q$  is the scale of the hard process and  $m$  is the charged particle mass.

But since there only hard processes with photon emission are considered these arguments do not apply to our case. We consider exclusive **soft process**  $pp \rightarrow ppy$  with soft photon emission.

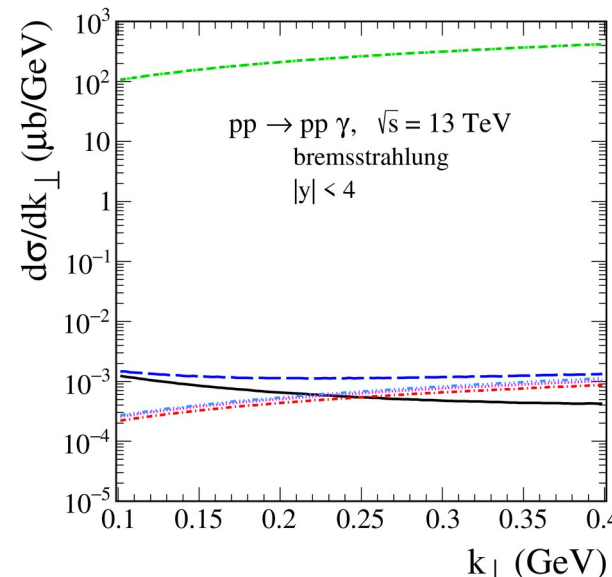
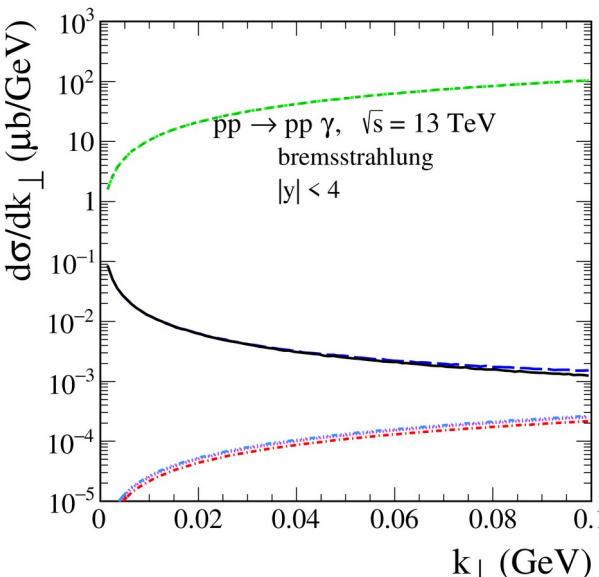
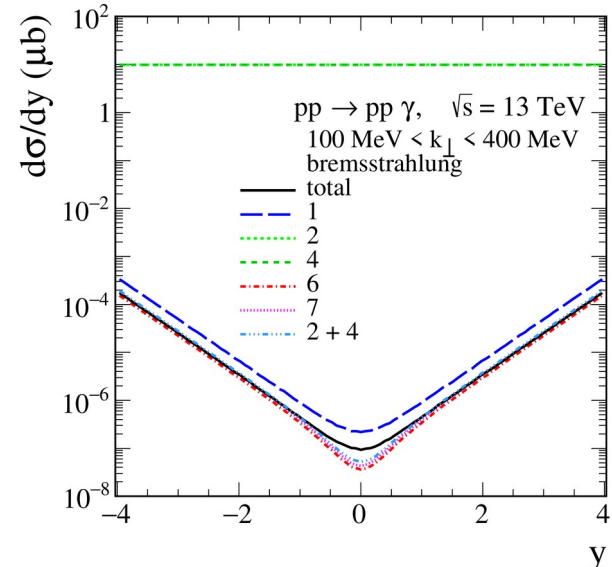
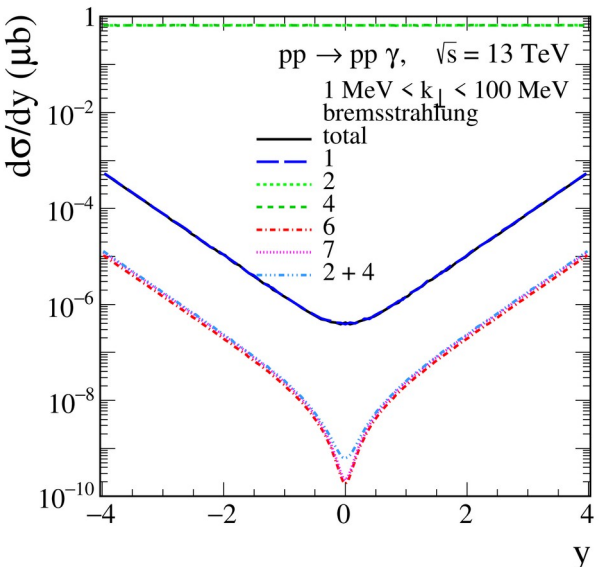
We have, of course, to take all contributions with different labels  $j$  into account and add them coherently.<sup>17</sup>



- We show the complete result (total) including interference effects and the results for individual  $j$  terms, except for  $j = 3$  and 5 which are very small and can be neglected. The coherent sum of the amplitudes with  $j = 2$  and 4 is denoted by  $2 + 4$ .
- There is significant cancellation among the terms  $j = 2$  and 4** due to destructive interference (not due to a gauge cancellation) and their sum is harmless, well below the term 1, at least for  $k_\perp < 100$  MeV and  $\omega < 2$  GeV.

This leads to a much larger region in  $k_\perp$  and  $\omega$  where the pole term ( $j = 1$ ) gives a good representation of the radiative amplitude.

- It is essential to add coherently all the various parts of the amplitude for soft photon emission in order not to miss important interference effects!



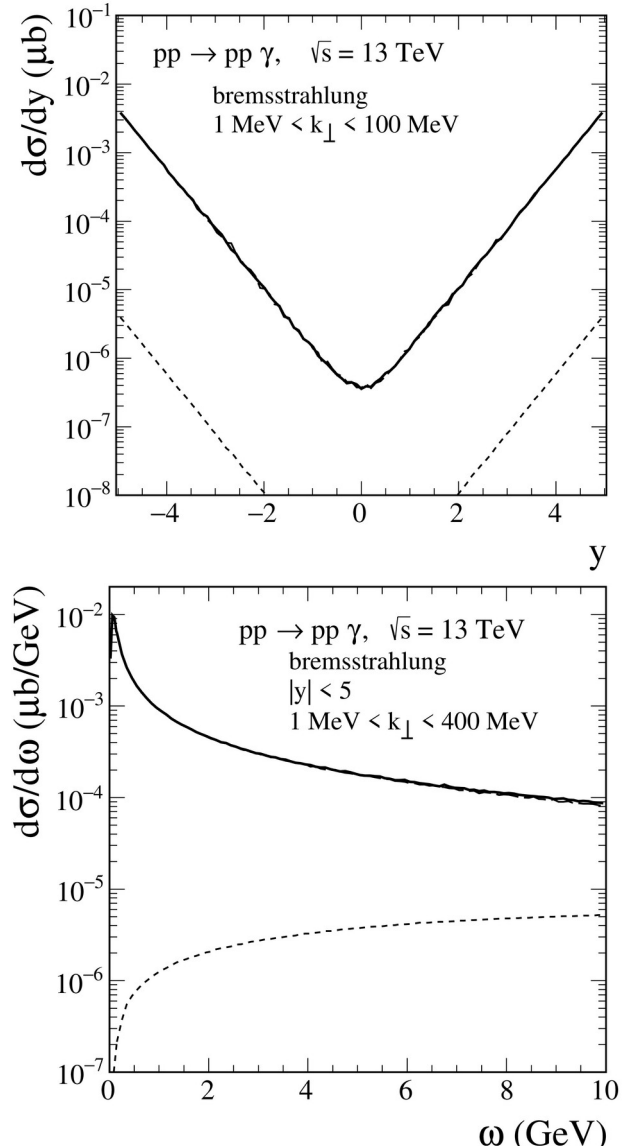
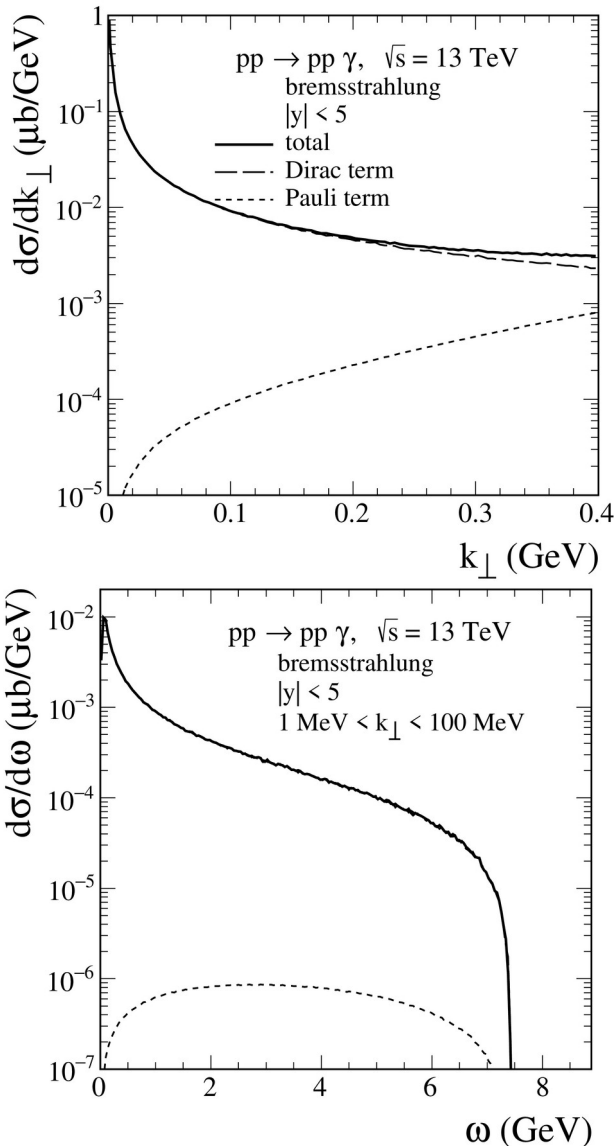
- In small  $k_\perp$  and  $\omega$  regions the Dirac term from  $\gamma pp$  vertex function dominates while for larger values the anomalous magnetic moment of the proton (Pauli term) plays an important role.

For the complete result all contributions to

$$\mathcal{M}_\mu^{(\text{standard})}$$

with Dirac and Pauli terms have to be added coherently.

- We get the integrated cross sections for  $\sqrt{s} = 13 \text{ TeV}$  and in the  $k_\perp$  range  $1 \text{ MeV} < k_\perp < 100 \text{ MeV}$ :  
 $\sigma = 0.21 \text{ nb}$  for  $|y| < 3.5$   
and  $\sigma = 4.01 \text{ nb}$  for  $3.5 < |y| < 5$ .



## Soft Photon Approximation (SPA)

We shall compare our “exact” model results, which we call “standard” to two SPAs.  
We consider only the pomeron-exchange.

**SPA 1** Here we keep only the pole terms  $\propto \omega^{-1}$  for  $\mathcal{M}_\mu^{(a)}, \dots, \mathcal{M}_\mu^{(f)}$ .

For real photons ( $k^2 = 0$ ), neglecting gauge terms  $\propto k_\mu$ , and with  $p'_1 \rightarrow p_1$ ,  $p'_2 \rightarrow p_2$  we get

$$\mathcal{M}_\mu \rightarrow \mathcal{M}_{\mu, \text{SPA1}} = e \mathcal{M}^{(\text{on shell}) pp}(s, t) \left[ -\frac{p_{a\mu}}{(p_a \cdot k)} + \frac{p_{1\mu}}{(p_1 \cdot k)} - \frac{p_{b\mu}}{(p_b \cdot k)} + \frac{p_{2\mu}}{(p_2 \cdot k)} \right]$$

- In the soft photon limit,  $\omega \rightarrow 0$ , the SPA amplitude can be factorized into the hadron part  $\mathcal{M}^{(\text{on shell})}$  and the photon emission part.

We get the following SPA1 result for the inclusive photon cross section where, for consistency, we neglect the photon momentum  $k$  in the energy-momentum conserving  $\delta^{(4)}(.)$  function

$$\begin{aligned} d\sigma(pp \rightarrow pp\gamma)_{\text{SPA1}} &= \frac{d^3k}{(2\pi)^3 2k^0} \int d^3p_1 d^3p_2 e^2 \frac{d\sigma(pp \rightarrow pp)}{d^3p_1 d^3p_2} \\ &\quad \times \left[ -\frac{p_{a\mu}}{(p_a \cdot k)} + \frac{p_{1\mu}}{(p_1 \cdot k)} - \frac{p_{b\mu}}{(p_b \cdot k)} + \frac{p_{2\mu}}{(p_2 \cdot k)} \right] \\ &\quad \times \left[ -\frac{p_{a\nu}}{(p_a \cdot k)} + \frac{p_{1\nu}}{(p_1 \cdot k)} - \frac{p_{b\nu}}{(p_b \cdot k)} + \frac{p_{2\nu}}{(p_2 \cdot k)} \right] (-g^{\mu\nu}) \\ \frac{d\sigma(pp \rightarrow pp)}{d^3p_1 d^3p_2} &= \frac{1}{2\sqrt{s(s - 4m_p^2)}} \frac{1}{(2\pi)^3 2p_1^0 (2\pi)^3 2p_2^0} (2\pi)^4 \delta^{(4)}(p_1 + p_2 - p_a - p_b) \frac{1}{4} \sum_{p \text{ spins}} |\mathcal{M}^{(\text{on shell}) pp}(s, t)|^2 \end{aligned}$$

Here we keep the correct energy-momentum conservation relation

$$p_a + p_b = p'_1 + p'_2 + k .$$

We consider again real photon emission,

$$\mathcal{M}_\mu \rightarrow \mathcal{M}_{\mu, \text{SPA2}} = \mathcal{M}_{\mathbb{P}, \mu}^{(a+b+c)1} + \mathcal{M}_{\mathbb{P}, \mu}^{(d+e+f)1} .$$

The amplitudes  $\mathcal{M}_{\mathbb{P}, \mu}^{(a+b+c)1}$  and  $\mathcal{M}_{\mathbb{P}, \mu}^{(d+e+f)1}$  contain the pole terms  $\propto \omega^{-1}$  for  $\omega \rightarrow 0$  and are separately gauge invariant.

## Comparison of our “exact” model or “standard” bremsstrahlung results with SPAs

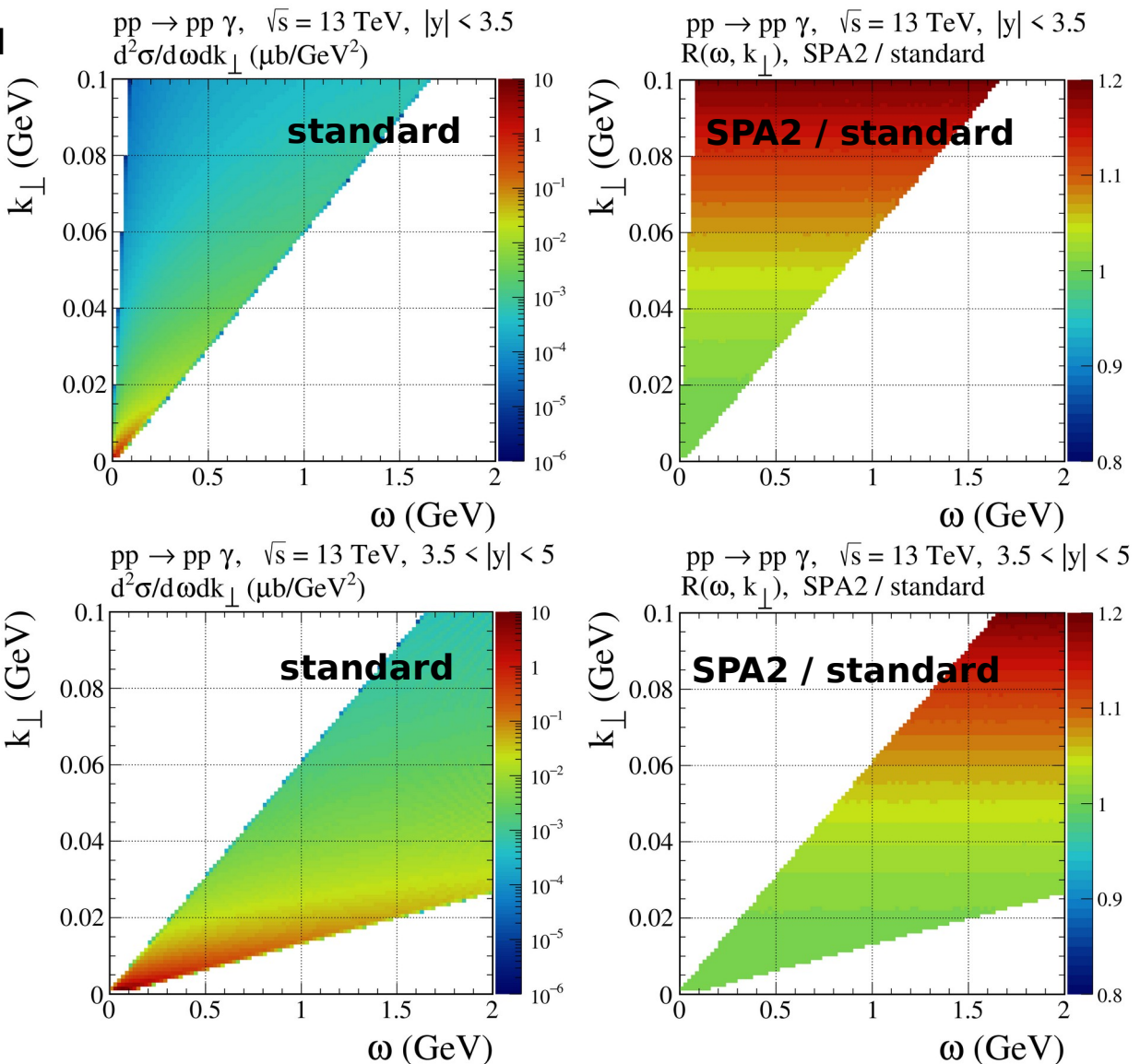
- In the left panels we show two-dimensional differential cross sections in the  $\omega$ - $k_{\perp}$  plane.

Large  $y$  is near the  $\omega$  axis, and  $y = 0$  corresponds to the line  $\omega = k_{\perp}$ , both in accordance with  $\omega = k_{\perp} \cosh y$ .

- In the right panels we show the ratio

$$R(\omega, k_{\perp}) = \frac{d^2\sigma_{\text{SPA2}}/d\omega dk_{\perp}}{d^2\sigma_{\text{standard}}/d\omega dk_{\perp}}$$

One can see that SPA2 stays within 1% accuracy for  $k_{\perp} < 22$  MeV and  $\omega < 0.35$  GeV considering  $|y| < 3.5$  and up to  $\omega \approx 1.7$  GeV for  $3.5 < |y| < 5.0$ .



## Comparison of “standard” results to SPA 1 and SPA 2

- (top panels)  
Both SPAs follow the standard results very well.

Surprisingly, the SPA 1 which does not have the correct energy-momentum relations fares somewhat better than SPA2.

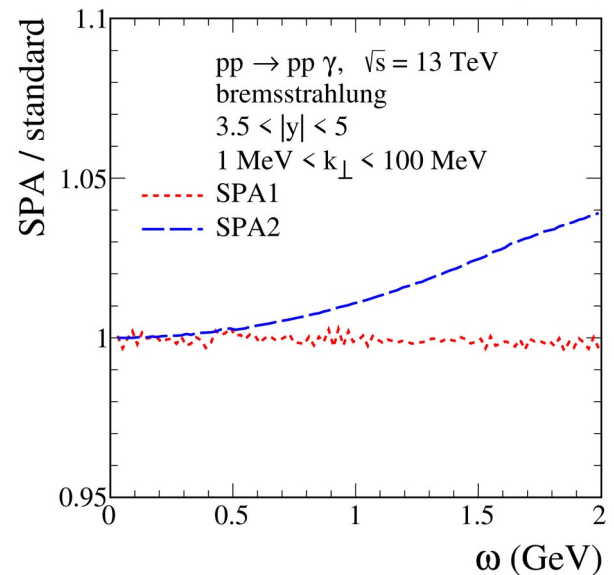
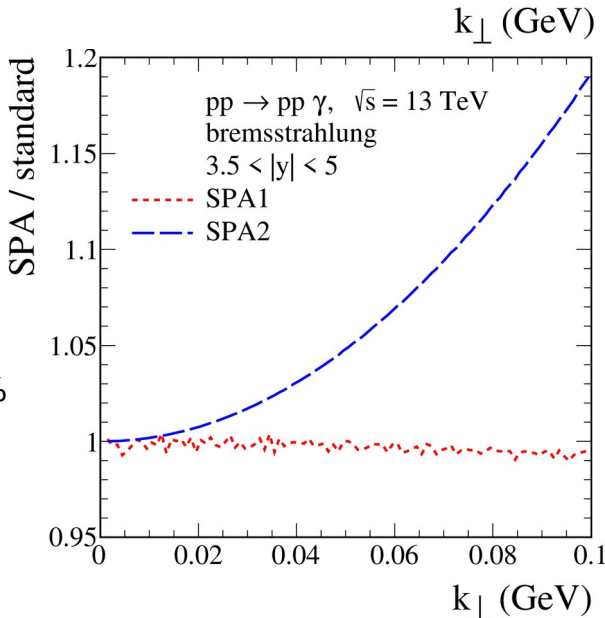
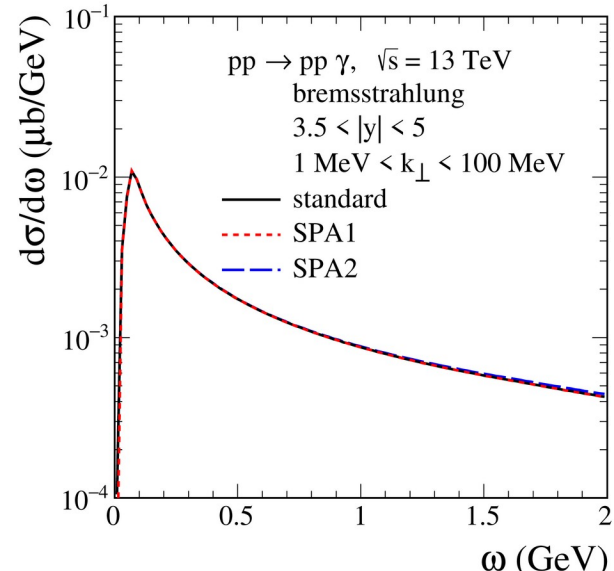
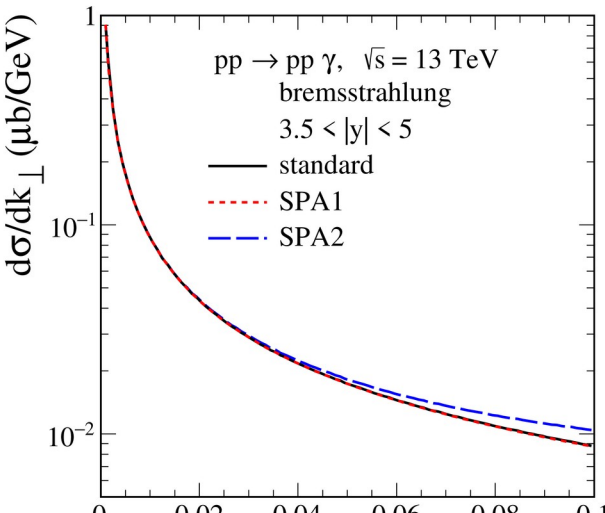
- (bottom panels)  
We show the ratios of the SPAs to the standard cross sections:

$$\frac{d\sigma_{\text{SPA}}/dk_\perp}{d\sigma_{\text{standard}}/dk_\perp} \quad \text{and} \quad \frac{d\sigma_{\text{SPA}}/d\omega}{d\sigma_{\text{standard}}/d\omega}$$

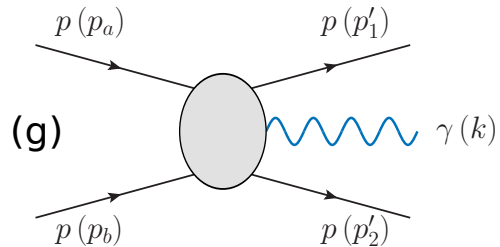
as function of  $k_\perp$  and  $\omega$ , respectively.

One can see that the deviations of the SPA1 from the standard results are up to around 1% in considered region.

For the SPA2 the deviations increase rapidly with growing  $k_\perp$  and  $\omega$ .

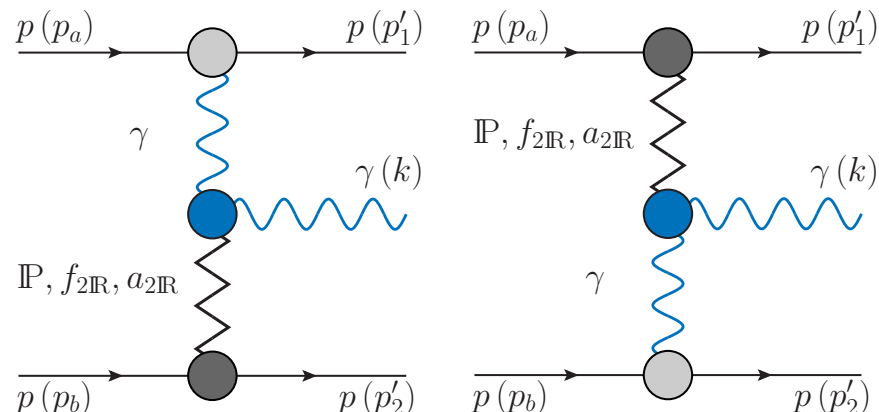


- Other contributions

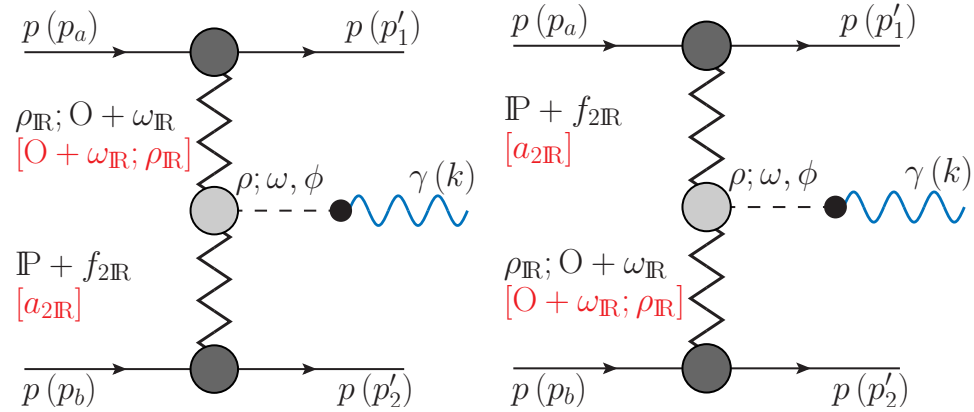


The amplitude must satisfy:  $k^\mu \mathcal{M}_\mu^{(g)} = 0$   
and has no singularity for  $k \rightarrow 0$ .

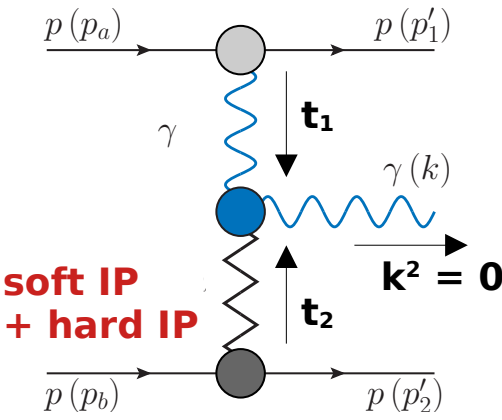
### Central exclusive production (CEP), fusion processes



$$\mathcal{M}_\mu^{(\gamma-\mathbb{P}/\mathbb{R})} = \mathcal{M}_\mu^{(\gamma\mathbb{P})} + \mathcal{M}_\mu^{(\mathbb{P}\gamma)} + \mathcal{M}_\mu^{(\gamma\mathbb{R}+)} + \mathcal{M}_\mu^{(\mathbb{R}+\gamma)}$$



Here we assume the VMD relations in the  $V \rightarrow \gamma$  vertices.  
Vertices occurring here are discussed in:  
[Ewerz, Maniatis, Nachtmann, Ann. Phys. 342 \(2014\) 31, PL, Nachtmann, Szczerba, PRD 101 \(2020\) 094012](#)



The Ansatz for the  $\text{IP}\gamma\gamma$  coupling functions for both real and virtual photons is discussed in [Britzger, Ewerz, Glazov, Nachtmann, Schmitt, PRD 100 \(2019\) 114007](#).

The coupling functions  $\hat{a}$  and  $\hat{b}$  were determined from the global fit to HERA inclusive DIS data and the total photoproduction cross section  $\sigma_{\gamma p}$ , and from HERA DVCS data.

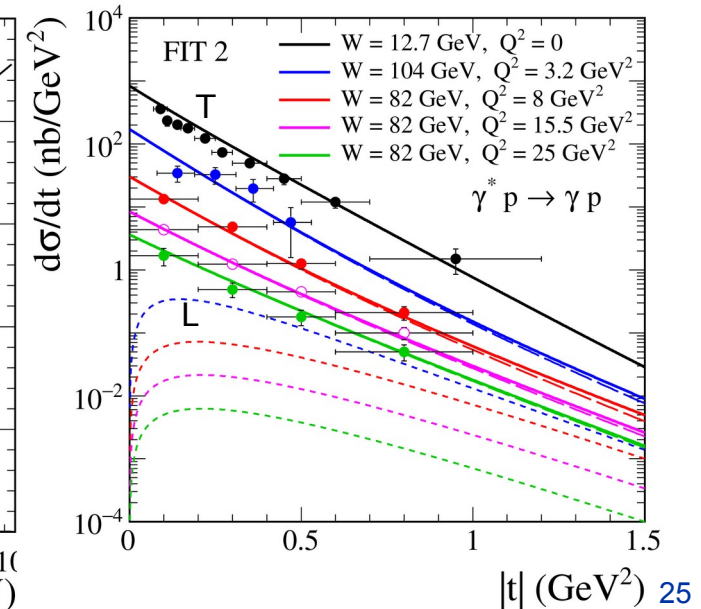
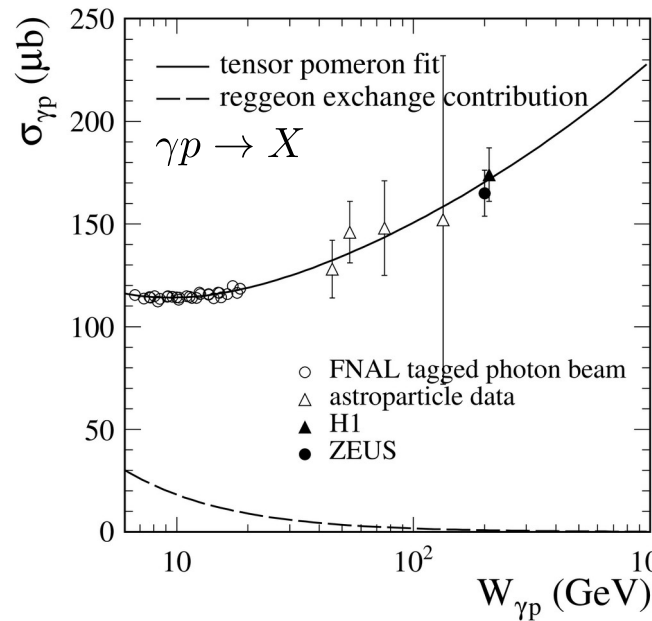
The  $t$  dependence of  $\gamma p$  subsystem is from fit of the model to the FNAL data on real Compton scattering  $\gamma p \rightarrow \gamma p$  (and also to DVCS HERA data)

$$\begin{aligned} F_{\text{eff}}^{(\mathbb{P})}(t) &= F^{(\mathbb{P}\gamma\gamma)}(t) \times F^{(\mathbb{P}pp)}(t) \\ &= \exp(-b_{\text{eff}}|t|/2) \end{aligned}$$

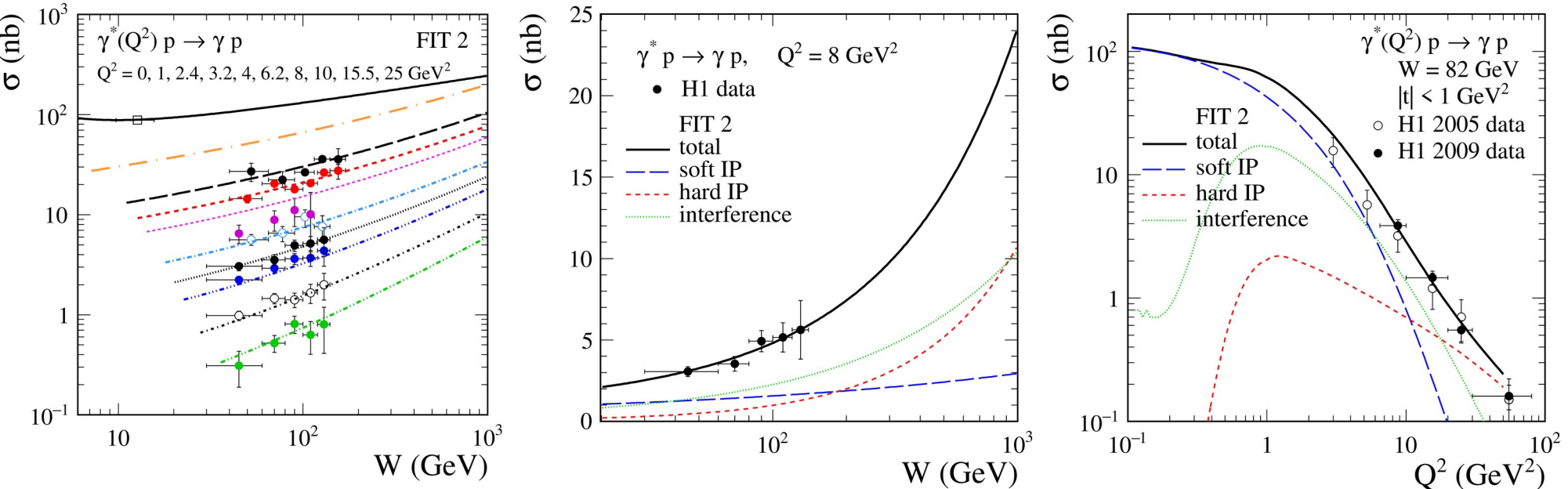
The  $\gamma\mathbb{P}$ -exchange amplitude can be written as

$$\begin{aligned} \mathcal{M}_{\mu}^{(\gamma\mathbb{P})} &= (-i) \bar{u}_{1'} i\Gamma_{\nu_1}^{(\gamma pp)}(p'_1, p_a) u_a i\Delta^{(\gamma)\nu_1\nu}(q_1) i\Gamma_{\mu\nu\kappa\rho}^{(\mathbb{P}\gamma^*\gamma)}(k, q_1) i\Delta^{(\mathbb{P})\kappa\rho,\alpha\beta}(s_2, t_2) \\ &\quad \times \bar{u}_{2'} i\Gamma_{\alpha\beta}^{(\mathbb{P}pp)}(p'_2, p_b) u_b \\ &= \bar{u}_{1'} \Gamma^{(\gamma pp)\nu}(p'_1, p_a) u_a \frac{1}{t_1} \frac{1}{2s_2} (-is_2\alpha'_{\mathbb{P}})^{\alpha_{\mathbb{P}}(t_2)-1} \bar{u}_{2'} \Gamma_{\alpha\beta}^{(\mathbb{P}pp)}(p'_2, p_b) u_b \\ &\quad \times i [2a_{\mathbb{P}\gamma^*\gamma}(t_1, k^2, t_2) \Gamma_{\mu\nu}^{(0)\alpha\beta}(k, -q_1) - b_{\mathbb{P}\gamma^*\gamma}(t_1, k^2, t_2) \Gamma_{\mu\nu}^{(2)\alpha\beta}(k, -q_1)] \end{aligned}$$

dominant term:  $b_{\mathbb{P}\gamma^*\gamma}(-Q_1^2, 0, t_2) = e^2 \hat{b}_{\mathbb{P}}(Q_1^2) F^{(\mathbb{P}\gamma\gamma)}(t_2)$   
where  $Q_1^2 = -t_1$  is the photon virtuality

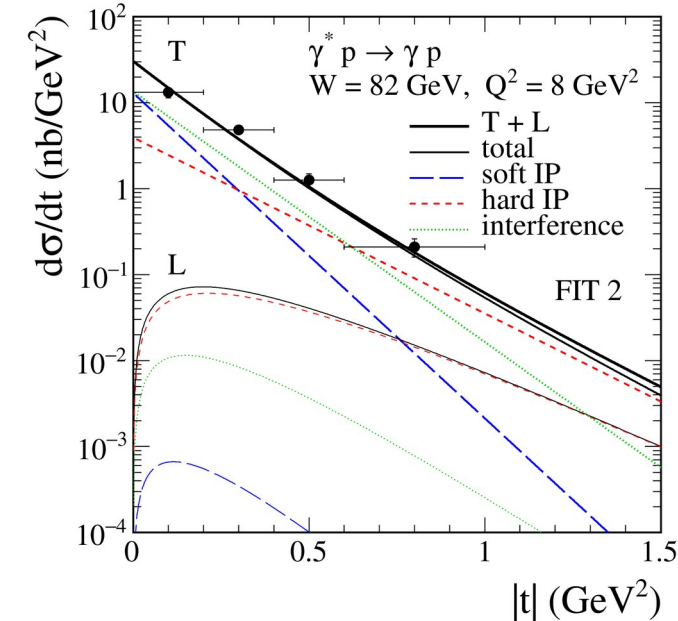
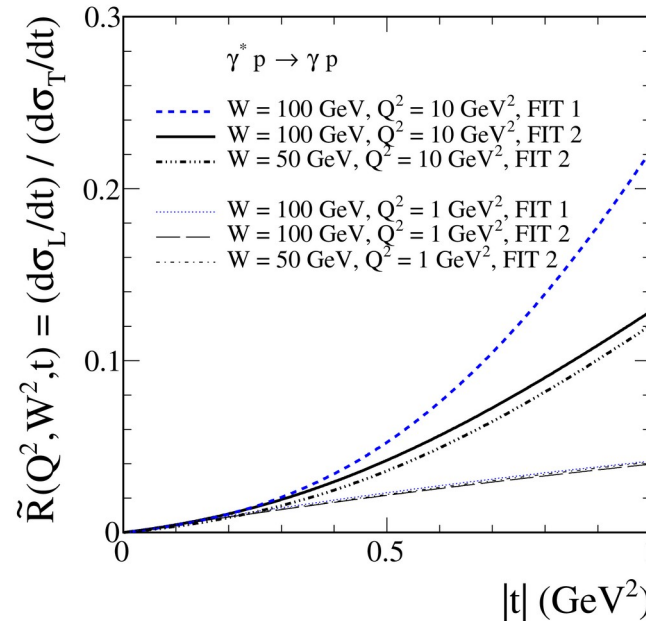
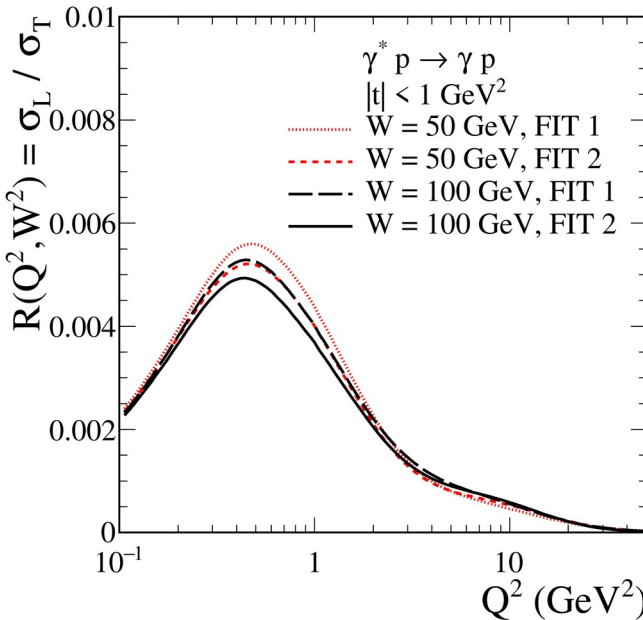


- **Comparison of two-tensor pomeron model with DVCS data**



- This Regge type model can be used for large energy  $W$ ,  $|t| \leq 1 \text{ GeV}^2$ , and small Bjorken- $x$ , say  $x \approx Q^2 / W^2 < 0.02$
- For real Compton scattering ( $Q^2 = 0$ ) the cross section is dominated by soft-pomeron exchange with an additional contribution from reggeon exchange at lower energies  $W$ .
- For higher  $W$ , the contribution from the hard pomeron is enhanced, gives a steeper rise of the cross section with  $W$  ( $\sigma \propto W^{2\epsilon}$ ,  $\epsilon_{\text{softIP}} \approx 0.09 < \epsilon_{\text{hardIP}} \approx 0.3$ ) and especially so for larger  $Q^2$ .
- For higher  $Q^2$  the soft component slowly decreases relative to the hard one.  
A significant constructive interference effect between soft and hard components is clearly visible  
(see also, e.g., Fazio, Fiore, Jenkovszky, Salii, PRD90 (2014) 016007 where also Regge theory is applied to DVCS)

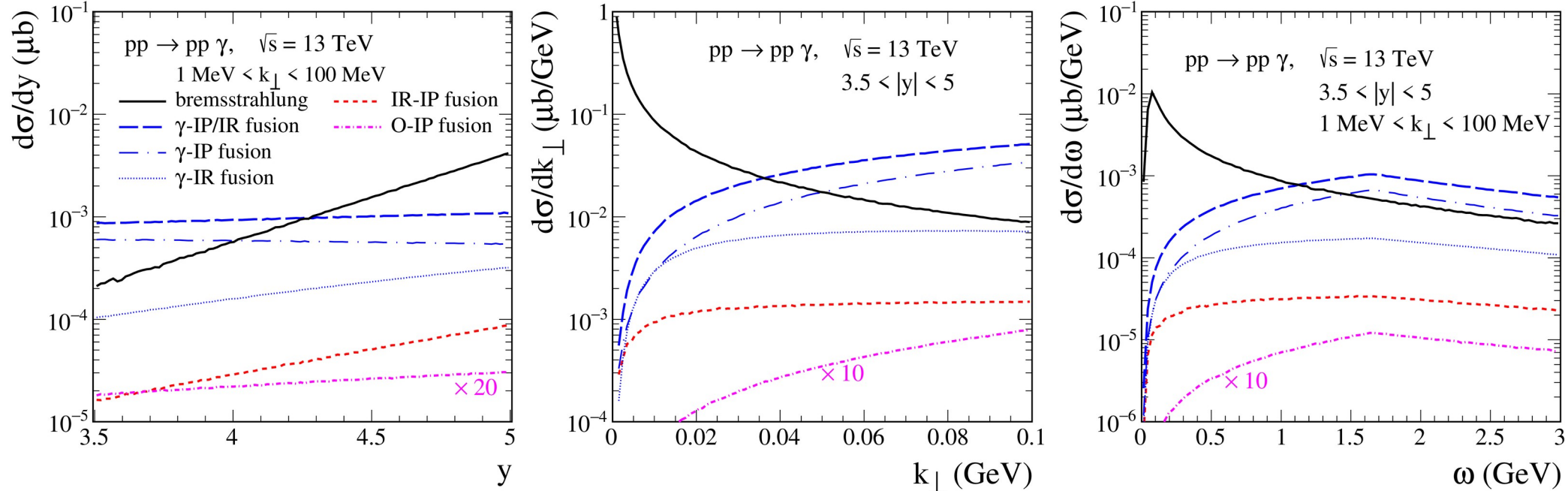
- Comparison of two-tensor pomeron model with DVCS data



- The ratios of the  $\gamma^* p \rightarrow \gamma p$  cross sections for longitudinally and transversely polarized virtual photons as functions of  $Q^2$  and  $|t|$ . The ratio  $\tilde{R}$  strongly grows with  $|t|$ ; this behaviour depends on our assumption that a and b couplings of IP $\gamma^*\gamma^*$  vertex functions have the same  $t$  dependence
- The slope parameters  $b_2$  (reggeon) and  $b_1$  (soft IP) are adjusted to the FNAL  $d\sigma/dt$  data on the real-photon-proton scattering. At higher  $W$  and  $Q^2$  the hard IP plays an increasingly important role.  
The slope parameter  $b_0$  for the hard-IP exchange is adjusted to the DVCS HERA data ( $b_0 < b_1$ ).
- $d\sigma/dt = d\sigma_T/dt + d\sigma_L/dt$  with the latter term becoming very small for  $|t| \rightarrow 0$ .  
 $d\sigma_T/dt$  is dominated by the b-type couplings and  $d\sigma_L/dt$  is dominated by the a-type couplings
- Our complete result for  $d\sigma/dt$  does not have a simple exponential  $t$  dependence. This is caused by the interference of soft- and hard-pomeron terms (each with different  $t$  dependence) and by the L contribution

- Comparison of diffractive bremsstrahlung to CEP fusion processes for ALICE 3 kinematics

Preliminary results!  $3.5 < |y| < 5.0$  and  $1 \text{ MeV} < k_{\perp} < 100 \text{ MeV}$

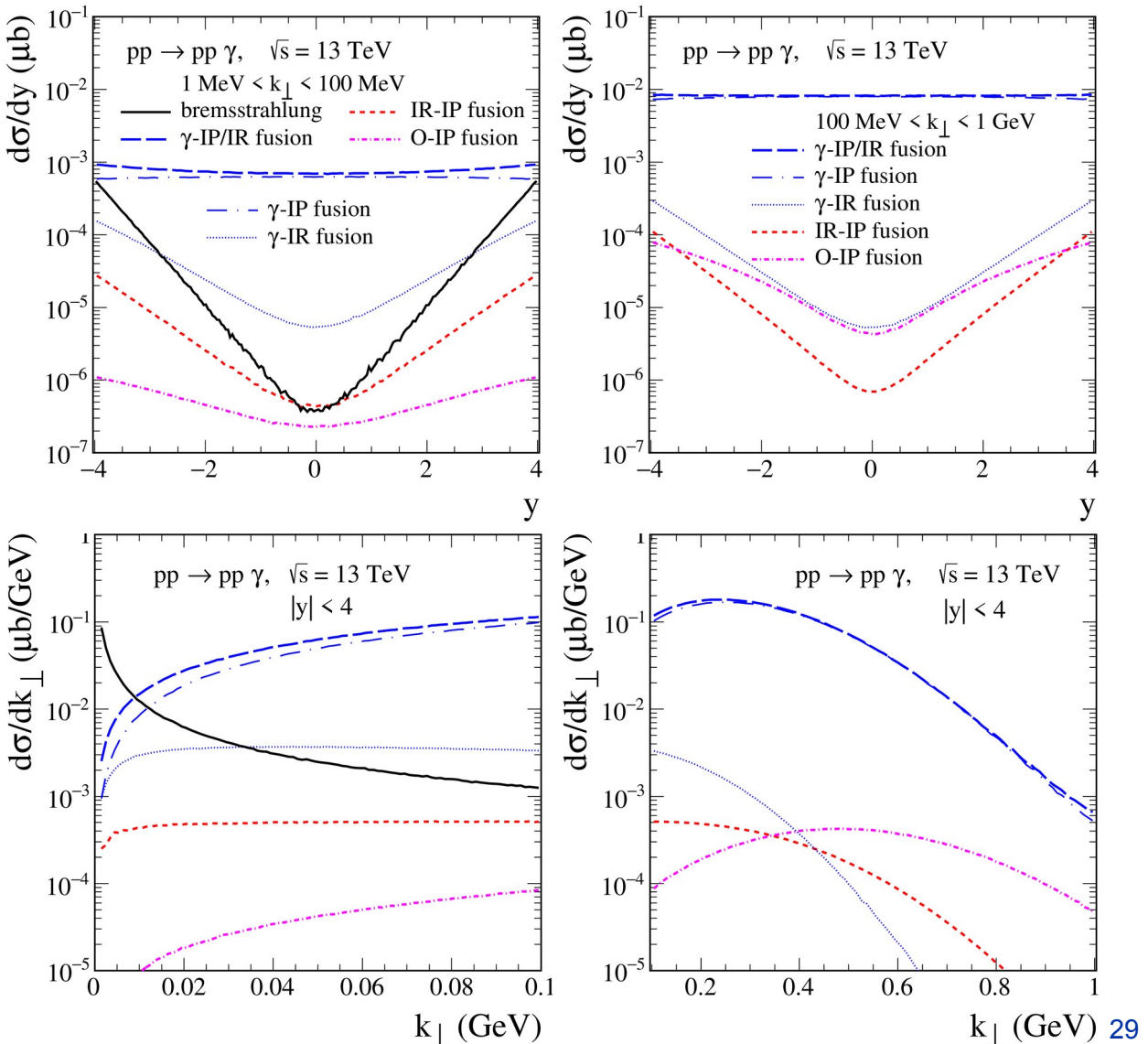


- Diffractive bremsstrahlung wins with CEP fusion processes in the soft-photon limit  $k_{\perp} \rightarrow 0$  and for large  $|y|$
- The bremsstrahlung via the  $\gamma$  exchange (QED process) is about a factor 200 smaller than the diffractive one
- The  $\gamma$ -IP/IR contributions are important in midrapidity region,  $|y| < 4.3$ , and  $k_{\perp} > 35 \text{ MeV}$ ,  $\omega > 1 \text{ GeV}$ . The purely diffractive IR-IP and O-IP contributions give much smaller cross section there.

## Preliminary results!

$|y| < 4$   
 $1 \text{ MeV} < k_{\perp} < 100 \text{ MeV}$  (left)  
 $100 \text{ MeV} < k_{\perp} < 1 \text{ GeV}$  (right)

- Photoproduction is very important at midrapidity region and large  $k_{\perp}$
- Absorption effects due to strong proton-proton interactions and possible interference effects between various mechanisms should be included



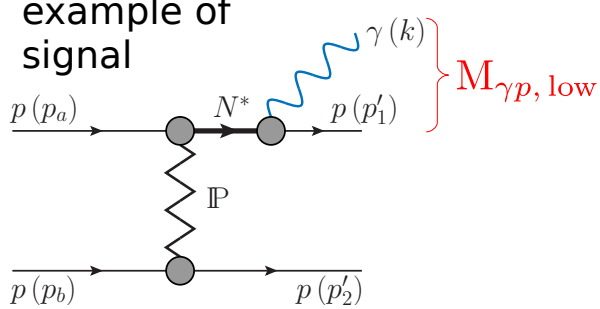
## Conclusions

- We constructed a model for the  $pp \rightarrow pp\gamma$  reaction for high energies and small momentum transfers using the tensor-pomeron approach.  
The amplitudes corresponding to photon emission from the external proton lines are determined by the off-shell  $pp \rightarrow pp$  scattering amplitude. By construction, the contact terms have to satisfy gauge-invariance constraints involving the previous amplitudes.
- We have taken care to write the formulas for the  $pp \rightarrow pp\gamma$  amplitude in such a way that they also apply to soft-virtual photon production, for instance,  $pp \rightarrow pp(\gamma^* \rightarrow e^+e^-)$ .
- We compared our “exact” or complete model results to SPA results.  
For the region  $1 \text{ MeV} < k_\perp < 100 \text{ MeV}$  and  $3.5 < |y| < 5.0$  (ALICE 3) we find that the SPA1 ansatz with only the pole terms  $\propto \omega^{-1}$  agrees at the percent level with our complete model result up to  $\omega \cong 2 \text{ GeV}$ .
- We are looking forward to further tests of non-perturbative QCD dynamics embodied in our tensor-pomeron exchanges in future electron-hadron collisions in the low-x regime at the EIC and LHeC colliders.

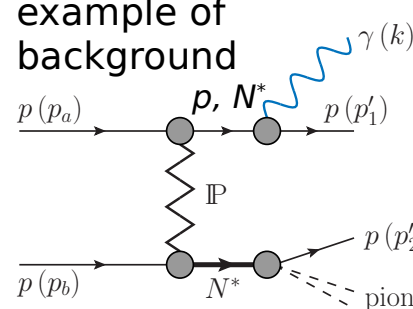
Thank you for listening !

## Comments on diffractive excitations of the protons ( $N^*$ resonances)

example of signal



example of background



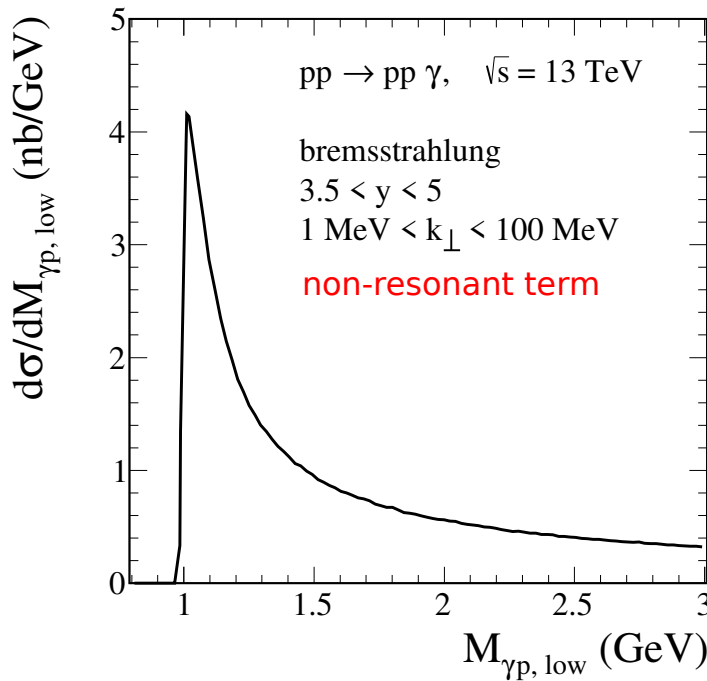
- $N^*$  candidates are (satisfy the Gribov-Morrison rule):  
 $N(1440) J^P=1/2^+$ ,  $N(1520) J^P=3/2^-$ ,  $N(1680) J^P=5/2^+$

$$\text{BR}(N(1440) \rightarrow p\gamma) \sim 0.04 \%$$

$$\text{BR}(N(1520) \rightarrow p\gamma) \sim 0.3 - 0.5 \%$$

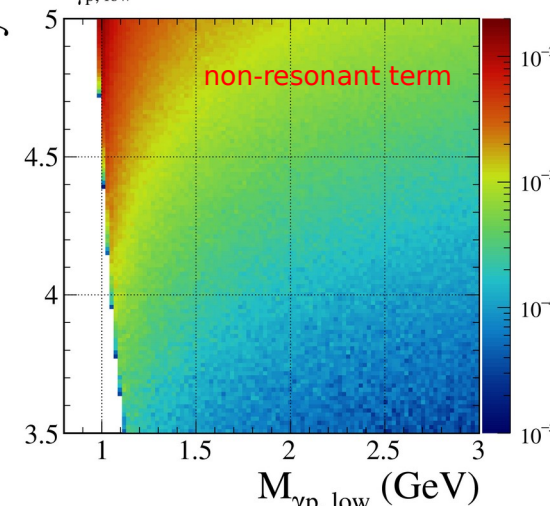
$\text{BR}(N(1680) \rightarrow p\gamma) \sim 0.2 - 0.3 \% \leftarrow$  a sizeable cross section  
 $pp \rightarrow pN(1680)$  was estimated at CERN ISR @ 45 GeV

- If these processes contribute significantly to our reaction then we should see them in the  $M_{\gamma p, \text{low}}$  distribution (possibly distorted by interference effects) as a resonance enhancement at  $M_{\gamma p} = m_{N^*}$  over the non-resonant term



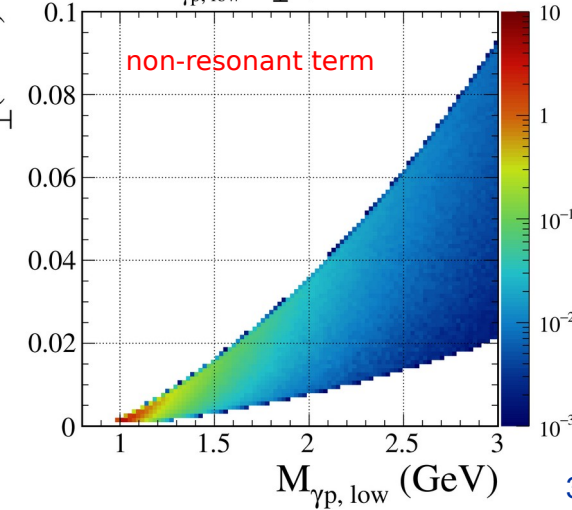
$pp \rightarrow pp\gamma, \sqrt{s} = 13 \text{ TeV}, 1 \text{ MeV} < k_\perp < 100 \text{ MeV}$

$d^2\sigma/dM_{\gamma p, \text{low}} dy (\mu\text{b}/\text{GeV})$



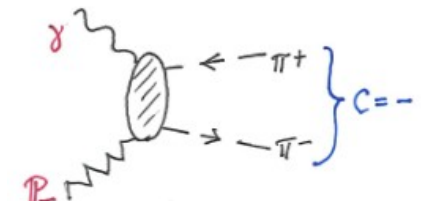
$pp \rightarrow pp\gamma, \sqrt{s} = 13 \text{ TeV}, 3.5 < y < 5$

$d^2\sigma/dM_{\gamma p, \text{low}} dk_\perp (\mu\text{b}/\text{GeV}^2)$

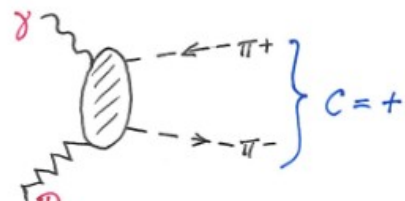


# Applications of the tensor-pomeron model

- **Photoproduction and low  $x$  DIS** *Britzger, Ewerz, Glazov, Nachtmann, Schmitt, PRD100 (2019) 114007*  
“vector IP” decouples completely in the total photoabsorption cross section and in the structure functions of DIS
- **$\gamma p \rightarrow \pi^+ \pi^- p$**  *Bolz, Ewerz, Maniatis, Nachtmann, Sauter, Schöning, JHEP 01 (2015) 151*  
interference between  $\gamma p \rightarrow (\rho^0 \rightarrow \pi^+ \pi^-) p$  (pomeron exch.) and  $\gamma p \rightarrow (f_2(1270) \rightarrow \pi^+ \pi^-) p$  (odderon exch.)  $\rightarrow \pi^+ \pi^-$  charge asymmetries



$\pi^+ \pi^-$  in antisymmetric state



$\pi^+ \pi^-$  in symmetric state

For a tensor (vector) pomeron the  $\pi^+ \pi^-$  pair is in antisymmetric (symmetric) state under the exchange  $\pi^+ \leftrightarrow \pi^-$ . Since the pomeron has  $C = +1$  the  $\pi^+ \pi^-$  pair must be in antisymmetric state. This gives a further clear evidence against a vector nature of the pomeron.

- **Central Exclusive Production (CEP),  $p p \rightarrow p p$**  *X, P.L., Nachtmann, Szczurek:*

*X:  $\eta, \eta', f_0(980), f_0(1370), f_0(1500)$  Ann. Phys. 344 (2014) 301*

$\rho^0$  *PRD91 (2015) 074023*

$\pi^+ \pi^-$  continuum,  $f_2(1270) \rightarrow \pi^+ \pi^-$  *PRD93 (2016) 054015, PRD101 (2020) 034008*

$\pi^+ \pi^- \pi^+ \pi^-$ ,  $\rho^0 \rho^0$  *PRD94 (2016) 034017*

$\rho^0$  with proton diss. *PRD95 (2017) 034036*

$p\bar{p}$  *PRD97 (2018) 094027*

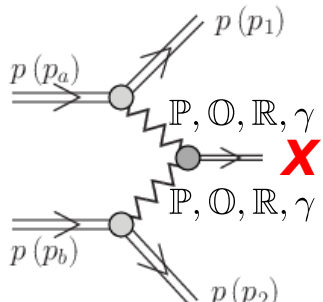
$K^+ K^-$  *PRD98 (2018) 014001*

$\phi \rightarrow K^+ K^-, \mu^+ \mu^-$  *PRD101 (2020) 094012*

$\phi \phi \rightarrow K^+ K^- K^+ K^-$  *PRD99 (2019) 094034*

$f_1(1285), f_1(1420)$  *P.L., Leutgeb, Nachtmann, Rebhan, Szczurek, PRD102 (2020) 114003*

$K^{*0} \bar{K}^{*0}$  continuum vs  $f_2(1950)$  *P.L., PRD103 (2021) 054039*



} odderon exchange

# Applications of the tensor-pomeron model

- Helicity in proton-proton elastic scattering and the spin structure of the soft pomeron**

Ewerz, P.L., Nachtmann, Szczerba, PLB 763 (2016) 382

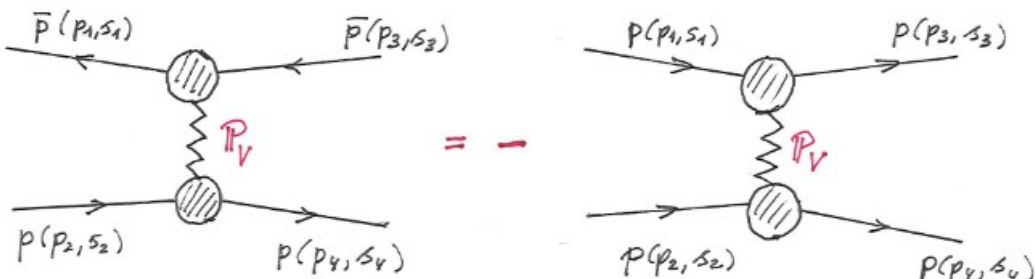
Studying the ratio  $r_5$  of single-helicity-flip to non-flip amplitudes we found that the STAR data are compatible with the tensor pomeron ansatz while they exclude a scalar character of the pomeron (the scalar-pomeron result is far outside the experimental error ellipse).

$$r_5(s, t) = \frac{2m_p \phi_5(s, t)}{\sqrt{-t} \operatorname{Im}[\phi_1(s, t) + \phi_3(s, t)]}$$

$$r_5^{P_T}(s, t) = -\frac{m_p^2}{s} \left[ i + \tan \left( \frac{\pi}{2} (\alpha_{PT}(t) - 1) \right) \right], r_5^{P_T}(s, 0) = (-0.28 - i2.20) \times 10^{-5}$$

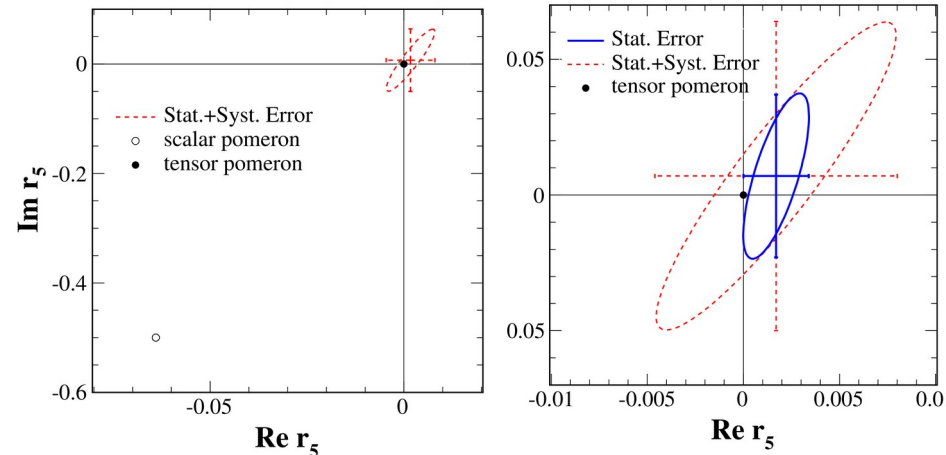
$$r_5^{P_S}(s, t) = -\frac{1}{2} \left[ i + \tan \left( \frac{\pi}{2} (\alpha_{PS}(t) - 1) \right) \right], r_5^{P_S}(s, 0) = -0.064 - i0.500$$

Problem with the vector pomeron:



STAR data: Adamczyk et al., PLB 719 (2013) 62  
[single spin asymmetry  $A_N$  in polarised  $pp \rightarrow pp$ ]

$\sqrt{s} = 200 \text{ GeV}, \quad 0.003 \leq |t| \leq 0.035 \text{ GeV}^2$



$$\sigma_{tot}^{pp} = \frac{1}{2\sqrt{s(s-4m_p^2)}} \operatorname{Im} [\phi_1(s, 0) + \phi_3(s, 0)]$$

Vector exchange has  $C = -1$ .  
It follows

$$\sigma_{tot}^{pp}|_{IP_V} = -\sigma_{tot}^{pp}|_{IP_V}$$

In our opinion a **vector pomeron is not a viable option**.

- *P.L. O. Nachtmann, A. Szczerba, PRD 105 (2022) 014022, arXiv:2107.10829*  
Considerations concerning the amplitude for the reaction  $\pi \pi^0 \rightarrow \pi \pi^0 \gamma$  in the soft-photon limit,  $\omega \rightarrow 0$ .

Using only rigorous QFT methods (no model dependence is contained there) we have calculated the terms of order  $\omega^{-1}$  and  $\omega^0$  in the expansion of the radiative amplitude.  
Our term of order  $\omega^0$  disagrees with that given by Low. We have analyzed this important discrepancy.  
→ Low's result corresponds to the expansion of the photon emission amplitude  
of the fictitious process  $\pi \pi^0 \rightarrow \pi \pi^0 \gamma$  where energy-momentum conservation is not respected

- From the theory side, we have a good model for the basic  $\pi\pi \rightarrow \pi\pi$  process.  
This allowed us to construct standard amplitude for  $\pi\pi \rightarrow \pi\pi\gamma$  (without anomalous terms).  
The terms  $\omega^{-1}$  and  $\omega^0$  in the expansion of standard amplitude are strict results from QFT without approximations, given the on-shell  $\pi\pi \rightarrow \pi\pi$  amplitudes.

Suppose now that we have experimental measurement of photon energies  $\omega$ .

If QFT describes experiment we must have for the ratio  $R_{\text{exp}}(\omega) = \frac{d\sigma_{\text{exp}}/d\omega}{d\sigma_{\text{standard}}/d\omega}$

$$\lim_{\omega \rightarrow 0} R_{\text{exp}}(\omega) = 1, \quad \lim_{\omega \rightarrow 0} \frac{dR_{\text{exp}}(\omega)}{d\omega} = 0.$$

A violation of these relations would mean a terrible crisis for QFT!  
For higher  $\omega$  a value  $R_{\text{exp}}(\omega) \neq 1$  would mean that there are soft photons from “anomalous” terms present in experiment.